

Archaeological and Anthropological Sciences

MORTARS AND PLASTERS - HOW TO CHARACTERISE AERIAL MORTARS AND PLASTERS

--Manuscript Draft--

Manuscript Number:	AASC-D-21-00022R3	
Full Title:	MORTARS AND PLASTERS - HOW TO CHARACTERISE AERIAL MORTARS AND PLASTERS	
Article Type:	Review	
Corresponding Author:	Duygu Ergenç, Ph.D. Instituto de Geociencias Madrid, Madrid SPAIN	
Corresponding Author Secondary Information:		
Corresponding Author's Institution:	Instituto de Geociencias	
Corresponding Author's Secondary Institution:		
First Author:	Duygu Ergenç, Ph.D.	
First Author Secondary Information:		
Order of Authors:	Duygu Ergenç, Ph.D.	
	Rafael Fort, Ph.D	
	Maria J. Varas-Muriel, Ph.D	
	Monica Alvarez de Buergo, Ph.D	
Order of Authors Secondary Information:		
Funding Information:	Ministerio de Economía, Industria y Competitividad, Gobierno de España (BIA2014-53911-R)	Dr. Rafael Fort
	Comunidad de Madrid (P2018/NMT-4372)	Dr. Rafael Fort
Abstract:	<p>Aerial mortars and plasters have been widely used in construction throughout history and their compatibility with historic mortars and plasters has led to their recent re-adoption. This paper reviews the prominent features of aerial mortars and plasters, their main characteristics and the various characterization methods using both traditional and advanced technology. Several techniques are used in physical, hydric, mechanical, petrographic, mineralogical and chemical characterization. A detailed explanation of microscopic characterization techniques is provided, indicating the information that can be obtained with each. Scientific advances in dating and provenance studies are also described.</p> <p>Keywords: aerial lime, physical-hydric-mechanical properties, petrographic, mineralogical, chemical, microscopic, isotopic characterization, dating techniques</p>	
Response to Reviewers:	Necessary additions are done in the final manuscript.	

MORTARS AND PLASTERS - HOW TO CHARACTERIZE AERIAL MORTARS AND PLASTERS

Information of authors:

DUYGU ERGENÇ

Department of Civil Engineering, Middle East Technical University, Ankara, Turkey

dergenc@metu.edu.tr, ORCID: 0000-0001-9034-1818

RAFAEL FORT

Instituto de Geociencias IGEO (CSIC-UCM), Spanish Research Council and Complutense University of Madrid, Madrid, Spain

rafael.fort@csic.es, ORCID: 0000-0001-9967-2824

MARIA J. VARAS-MURIEL

Instituto de Geociencias IGEO (CSIC-UCM), Spanish Research Council and Complutense University of Madrid, Madrid, Spain

School of Geology, Complutense University of Madrid (UCM), Madrid, Spain

mjvaras@ucm.es, ORCID: 0000-0002-0441-0811

MONICA ALVAREZ DE BUERGO

Instituto de Geociencias IGEO (CSIC-UCM), Spanish Research Council and Complutense University of Madrid, Madrid, Spain

monica.alvarez@igeo.ucm-csic.es, ORCID: 0000-0002-7520-2390

Abstract

Aerial mortars and plasters have been widely used in construction throughout history and their compatibility with historic mortars and plasters has led to their recent re-adoption. This paper reviews the prominent features of aerial mortars and plasters, their main characteristics and the various characterization methods using both traditional and advanced technology. Several techniques are used in physical, hydric, mechanical, petrographic, mineralogical and chemical characterization. A detailed explanation of microscopic characterization techniques is provided, indicating the information that can be obtained with each. Scientific advances in dating and provenance studies are also described.

Keywords: aerial lime, physical-hydric-mechanical properties, petrographic, mineralogical, chemical, microscopic, isotopic characterization, dating techniques

Funding: This research was funded by the CLIMORTEC (BIA2014-53911-R) project, Ministry of Economy and Competitiveness of Spain, and the TOP Heritage (P2018/NMT-4372) project, Community of Madrid.

Conflicts of interest/Competing interests: The authors have no conflicts of interest to declare

Availability of data and material: Not applicable

Code availability: Not applicable

MORTARS AND PLASTERS - HOW TO CHARACTERIZE AERIAL MORTARS AND PLASTERS

Duygu Ergenç¹, Rafael Fort², Maria J. Varas–Muriel^{2,3}, Monica Alvarez de Buergo²

¹ *Department of Civil Engineering, Middle East Technical University, Turkey*

² *Institute of Geosciences (IGEO), Spanish Research Council (CSIC) and Complutense University of Madrid (UCM), Spain*

³ *School of Geology, Complutense University of Madrid (UCM), Spain*

Email: dergenc@metu.edu.tr; rafael.fort@csic.es; mjvaras@ucm.es; monica.alvarez@csic.es

Outline

Abstract

1. Introduction

2. Principal properties of aerial lime mortars and plasters

3. How to characterize aerial lime mortars and plasters

3.1. Physical properties

3.2. Mechanical properties

3.3. Petrographic characterization

3.4. Mineralogical characterization

3.5. Chemical characterization

3.6. Stable Isotope analysis

3.7. Dating techniques

4. Final Remarks

References

Abstract

Aerial mortars and plasters have been widely used in construction throughout history and their compatibility with historic mortars and plasters has led to their recent re-adoption. This paper reviews the prominent features of aerial mortars and plasters, their main characteristics and the various characterization methods using both traditional and advanced technology. Several techniques are used in physical, mechanical, petrographic, mineralogical, and chemical characterization. A detailed explanation of microscopic characterization techniques is provided, indicating the information that can be obtained with each. Scientific advances in dating and provenance studies are also described.

Keywords: air-lime, physical-hydric-mechanical properties, petrographic, mineralogical, chemical, microscopic, isotopic characterization, dating methods

PREMISE

1 This Topical Collection (TC) covers several topics in the field of study, in which ancient architecture, art
2 history, archaeology and material analyses intersect. The chosen perspective is that of a
3 multidisciplinary scenario, capable of combining, integrating and solving the research issues raised by
4 the study of mortars, plasters and pigments.
5

6
7 The first group of contributions explains how mortars have been made and used through the ages
8 (Arizzi and Cultrone 2021, Lancaster 2021, Vitti 2021 and this paper). An insight into their production,
9 transport and on-site organisation is further provided by DeLaine (2021).
10

11
12 The second group of contributions is focused on pigments, starting from a philological essay on
13 terminology (Becker 2021). Three archaeological reviews on prehistoric (Domingo Sanz and Chieli
14 2021), Roman (Salvadori and Sbrolli 2021) and Medieval (Murat 2021) wall paintings clarify the
15 archaeological framework. A series of archaeometric reviews illustrate the state of the art of the
16 studies carried out on Fe-based red, yellow and brown ochres (Mastrotheodoros et al.
17 forthcoming), Cu-based greens and blues (Švarcová et al. 2021), as-based yellows and reds (Gliozzo
18 and Burgio 2021), lead-based whites, reds, yellows and oranges (Gliozzo and Ionescu 2021), Hg-based
19 red and white (Gliozzo 2021) and organic pigments (Aceto 2021). An overview of the use of inks,
20 pigments and dyes in manuscripts (Burgio 2021) and on glass-based pigments (Cavallo and Riccardi
21 forthcoming) is also presented. Furthermore, two papers on cosmetic (Pérez Arantegui 2021) and
22 medicinal pigments (Knapp et al. 2021) provide insights into the variety and different uses of these
23 materials.
24

25
26 Finally, several issues concerning the degradation and conservation of built heritage are addressed
27 from practical and technical standpoints (La Russa and Ruffolo 2021, Caroselli and Ruffolo 2021).
28
29
30
31
32

33 34 35 36 37 38 39 40 41 42 **1 INTRODUCTION**

43 44 45 46 **1.1 History and use**

47
48 Lime has been used for thousands of years as the binder in bedding, pointing and rendering mortars,
49 internal plaster, foundations, floors, wall infills and decorative elements (Elsen 2006). The first artificial
50 binders used by mankind were lime-based and gypsum-based plasters, which were employed widely
51 in the Middle East in the 7 and 8th millennia BC (Furlan and Bissegger 1975; Bensted 1997; Schmidt et
52 al 2011). Proof of the early use of lime is found in the plaster used to cover the walls and floors of
53 Göbekli Tepe in south-east Turkey (Hurd et al 2011; Artioli et al 2019). Lime mortar, however, was not
54 widely utilized until it was adopted by Greek and Roman builders and stonemasons in the 1st
55
56
57
58
59
60
61
62
63
64
65

1 millennium BC (Blezard 1998). The most important reference to lime mortar comes from Vitruvius's
2 *De Architectura*, written around 25 BC (Lancaster 2021). The main functions of aerial lime mortars were
3 as bonding for stones and bricks, as a render for protection and decoration (plaster) and as a
4 substratum layer for wall paintings, floors and mosaics (Borges et al 2014) (Figure 1a-b).
5

6 Lime can be considered, up to the arrival of natural and Portland cements in the late 18th and early 19th
7 centuries, respectively, the longest-lasting binder in the history of construction (Figure 1c-d). Today,
8 aerial lime is primarily used for repairs and is only employed in construction on a very small scale
9 (Carran et al 2012, Varas et al 2005, 2007).
10
11
12
13
14
15



55 Figure 1. Examples of aerial lime mortars/plasters in ancient and historic buildings in Spain. a) Wall
56 built with mortar and limestone pebbles (> 10 cm size) in the Roman city of Complutum, Madrid; b)
57 Part of a channel from the San Lázaro Roman aqueduct, Mérida; the base was built with aerial mortar
58 and limestone pebbles, with several layers of aerial and hydraulic rendering mortars; c) Various layers
59 of rendering mortars applied on a wall in the Monastery of Santa María la Real in Pelayos de la Presa,
60
61
62
63
64
65

1 Madrid, built in the 17th century; d) Detail of bedding mortar in brick masonry at the Cistercian
2 monastery of San Bernardo in Alcalá de Henares, Madrid, built between the 17th and 18th centuries.
3
4
5

6 1.2 Terminology 7

8 To avoid any terminological confusion, in this paper, and in accordance with EN 16572 (2015);
9

10 (a) the term **aggregate** indicates natural sediments and/or crushed rock fragments, or other man-
11 made/artificial materials, comprising a wide range of particle sizes and employed in mortar on the
12 one hand to provide strength and mechanical stability and durability and, on the other, to increase
13 workability. Regarding their grain size, they can be fine (e.g. sand, 0.063 mm to < 4 mm) or coarse
14 (e.g. gravel, > 4 mm);
15
16
17
18

19 (b) the term **binder** indicates the binding medium that, after hardening, holds the aggregate particles
20 together. It can be defined as a material with adhesive and cohesive properties capable of binding
21 aggregates into a coherent mass;
22
23

24 (b1) the term **lime** refers to a material composed of oxides (quicklime) or hydroxides (hydrated
25 or slaked lime) of calcium or of calcium and magnesium used as a binder.
26

27 (b2) the term **aerial lime** indicates a non-hydraulic lime that, when it hardens due to the
28 reaction with atmospheric carbon dioxide in the presence of humidity, transforms into a
29 carbonate.
30
31

32 (b3) **quicklime** is the product of calcination of limestone (at approximately 900 °C) and is
33 composed mainly of calcium oxides (CaO) or of calcium oxides combined with magnesium
34 oxides (MgO).
35
36
37

38 (b4) **slaked lime** is the viscous paste produced by hydrating quicklime (lime putty). Hydrated
39 lime refers to the solid powder produced by the same hydration reaction after dry-slaking
40 quicklime with just enough water to convert it. The composition may differ depending on the
41 mineralogical composition of the quicklime. If the quicklime is calcitic (CaO), calcium hydroxide
42 (Ca(OH)₂) – the mineralogical name of which is portlandite – is produced. Dolomitic limes,
43 which are rich in magnesium, produce Mg(OH)₂ in addition to Ca(OH)₂. The mineralogical name
44 of Mg(OH)₂ is brucite and it is obtained by hydrating (or slaking) dolomitic quicklime (CaO and
45 MgO) with water to produce a paste or powder.
46
47
48
49
50
51

52 (c) the term **mortar** indicates the hardened mixture of a viscous inorganic binder and aggregate.
53

54 (d) the term **plaster** indicates a coating composed of one or more layers of mortar applied in order of
55 execution and used on the internal surface of masonry; **render** (or **rendering**) refers to a coating
56 composed of one or more layers of mortar applied in order of execution and used on the external
57 surface of masonry to serve as a protective or surface finish.
58
59
60
61
62
63
64
65

1 (e) the term **additive** refers to a constituent usually added in small quantities to a mix to bind or modify
2 its manufacture or properties (e.g. air-entraining agents and setting accelerators); while the term
3 **admixture** indicates a substance other than binder, aggregate or water added to the mix in quantities
4 of at least 1% by weight to alter its properties (e.g. pigments, fibrous substances);
5

6
7 (f) **setting** is the process by which a mortar changes from a plastic, workable state to a stiffer, non-
8 workable state; **hardening** is the resistance acquired during and after the initial setting of the mortar;
9 and **curing** is the process by which mortars acquire strength due to carbonation, and when the process
10 is controlled by environmental conditions.
11

12 All the materials mentioned above have been processed and used as building materials to enhance
13 masonry's structural properties, diminish water contact, provide hygienic-sanitary protection
14 (limewash) during the epidemiological episodes that have affected human beings throughout history,
15 protect adjacent elements from direct exposure to weathering and to prepare the support for pictorial
16 decorations (Ergenç et al 2018a).
17

18 Mortars and plasters can be either aerial or hydraulic, depending on the type of binder used. While
19 hydraulic lime binders are produced using either impure carbonate or pure carbonate mixed with clays,
20 aerial lime binders are produced from pure carbonate (containing < 5% silicates) (EN 16572, 2015).
21

22 The lime cycle starts with calcination of limestone (CaCO_3), resulting in its decomposition to CaO .
23 Slaking then leads to calcium hydroxide (Ca(OH)_2 ; portlandite) formation and, with the final
24 carbonation process, the cycle ends with CaCO_3 . For a better understanding of binders and their
25 production process, as well as of the lime cycle, see Lancaster (2021, in this TC). Dolomitic lime has a
26 different cycle to calcitic lime. When dolostone (calcium and magnesium carbonate, $\text{CaMg(CO}_3)_2$) is
27 burnt, two-step decomposition occurs: firstly, dolomite decomposes into magnesium oxide (MgO ,
28 namely periclase), calcium carbonate (CaCO_3 , calcite) and calcium dioxide (CO_2); and secondly, calcium
29 carbonate decomposes into calcium oxide (CaO , quicklime) and calcium dioxide. In addition to
30 producing calcium hydroxide (Ca(OH)_2 , portlandite), the slaking process results in the formation of
31 magnesium hydroxide (Mg(OH)_2 , brucite), which is much more stable than portlandite, causing slow
32 carbonation that may be only partial. Therefore, the dolomitic lime cycle is not a full cycle like that
33 typical of lime (calcitic) (Beruto et al 2003; Ponce Antón et al 2018).
34
35
36
37
38
39
40
41
42
43
44
45
46
47
48
49
50
51
52
53
54

55 **2 PRINCIPAL PROPERTIES OF AERIAL MORTARS AND PLASTERS**

56 The best-known properties and behaviour of aerial lime mortars can be summarized as low
57 mechanical strength, high deformation capacity (plasticity), low elasticity modulus and high
58
59
60
61
62
63
64
65

1 permeability to water (in the liquid and gaseous state) due to their high porosity compared to hydraulic
2 lime mortars (Arandigoyen and Alvarez 2007). These mortars are not a source of detrimental salts
3 themselves. Their long setting times and low strength, when compared to hydraulic lime mortars, as
4 well as the loss of know-how and expertise regarding their manufacture, led to a decrease in their use,
5 especially in Europe. To enhance the properties of these mortars, inorganic and organic additives were
6 frequently incorporated into the mix to improve their carbonation speed, mechanical strength and
7 waterproofing performance (Sickels 1981; Carran et al 2012; Ventolà et al 2013; Veiga 2017). One of
8 the significant benefits of the manufacture of air-lime is its low environmental footprint in comparison
9 with hydraulic binders due to its high CO₂ sequestration capacity and the lower firing temperatures
10 reached in the kiln (less energy consumption), which makes it almost carbon-neutral and the most
11 environmentally friendly binder (Forster et al. 2020).

12 Other positive features of these mortars are their workability and plasticity (especially suited to
13 decorative finishes), which make them easy to apply and provide good adherence to the substrate
14 (Lawrence 2006; Veiga 2017).

25 **3 HOW TO CHARACTERIZE AERIAL MORTARS AND PLASTERS**

26 In the 19th century (1865), Wallace conducted one of the first studies of ancient mortars. He analysed
27 samples of mortars and plasters from ancient buildings in Egypt, Greece, Italy and Cyprus ranging in
28 age from 1500 to 3000 years old.

29 Much progress has been made in establishing standardized methodologies for analysing and
30 characterizing historic mortars thanks to the creation, for instance, of the RILEM (International Union
31 of Laboratories and Experts in Construction Materials, Systems and Structures) in 1947. The RILEM
32 created several key technical committees, among them *Technical Committee 167-COM: Characterization of historic mortars with respect to their repair*, as well as holding congresses (e.g.
33 Historic Mortar Conference) and issuing recommendations, reports and publications (Valek et al 2012;
34 Middendorf et al 2005).

35 More recently, the European Committee for Standardization has contributed significantly to this
36 progress, especially in the field of conservation of cultural heritage, by publishing standards regarding
37 terminology (EN 16572, 2015), the methodology for sampling (EN 16085, 2012), and different test
38 methods (EN 15801, 2009; EN 15803, 2009; EN 16302, 2013; EN 16322, 2013).

39 The latest European standard published (EN 17187:2020) establishes the methodology to be used to
40 characterize the mortars used in cultural heritage in order to define the petrographic, mineralogical,
41 chemical, physical and mechanical properties of these materials.

Best practice for improving the quality of characterization of aerial lime mortars consists of integrating all the information provided by multiple tests and analyses (Figure 2).

Sampling must be carried out in accordance with EN 16085 (2012), (Pizzo et al 2021, in this TC) for more detailed information about mortar sampling. EN 17187 (2020) presents flow charts and tables that facilitate selection of analytical methods for chemical, mineralogical, and petrographic characterization of mortars.

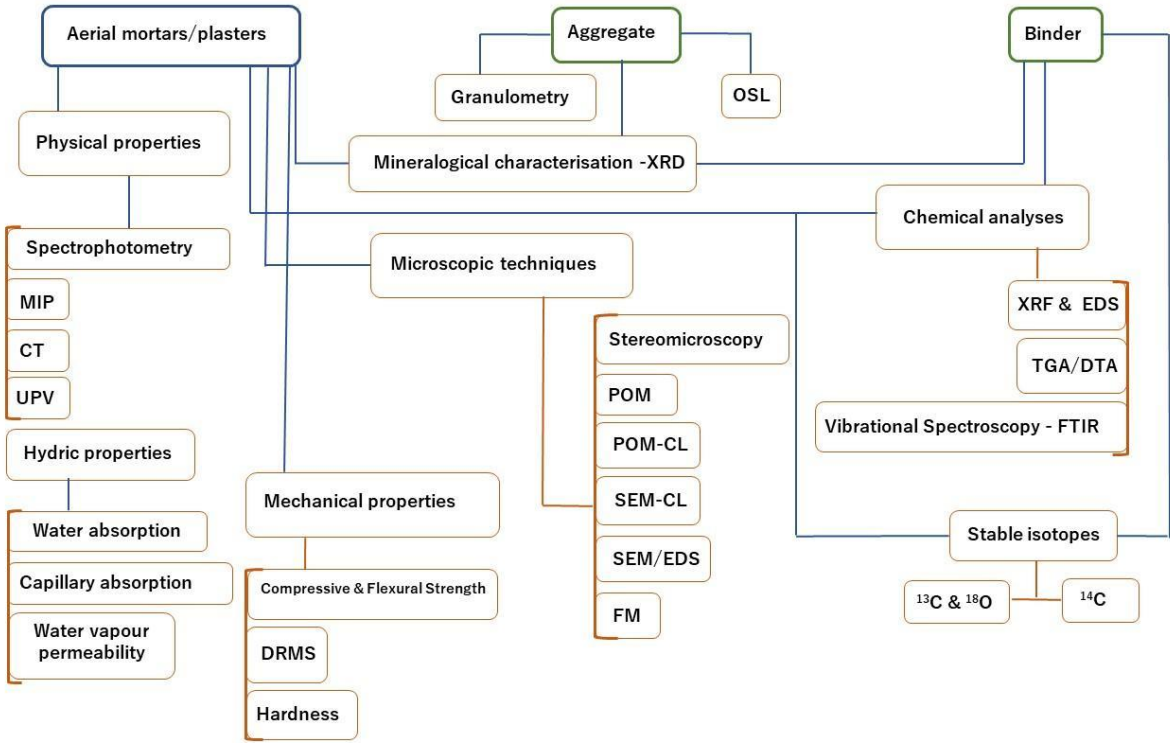


Figure 2. Chart showing characterization of aerial mortars/plasters, part of it adapted from EN 17187:2020 (CL: cathodoluminescence, CT: X-ray computed tomography, DRMS: drilling resistance measuring system, DTA: differential thermal analysis, EDS: energy-dispersive X-ray microanalysis, FM: fluorescence microscopy, FTIR: Fourier-transform infrared spectroscopy, MIP: mercury intrusion porosimetry, OSL: optically stimulated luminescence, POM: polarized optical microscopy, SEM: scanning electron microscopy, TGA: Thermogravimetric analysis, UPV: ultrasound pulse velocity, XRD: X ray diffraction, XRF: X ray fluorescence).

Any study of these mortars should begin with detailed macroscopic observation (EN 17187:2020) aided by a magnification loupe. Macroscopic study may provide information about the colour of the binder and aggregate, the presence or absence of lime lumps (nature, colour, size and distribution), nature, grain size, shape and distribution of the aggregate, existing porosity and its distribution, degree of

cohesion/adhesion between the components, stratigraphy of the mortar layers in the coatings, etc. (EN 17187:2020) (Figure 3).

In this stage of macroscopic survey, spraying a phenolphthalein ($C_{20}H_{14}O_4$) solution (14%) on air-lime mortars, and specifically on binder areas, provides a rapid, visual, and simple test frequently used (Cazalla et al. 2004; Lawrence 2006) to obtain an idea of the degree of binder carbonation, which is highly responsible for the final properties of aerial lime mortars. When phenolphthalein reacts with mediums with a pH of between 8.2 and 9.8, it turns magenta (where alkali $Ca(OH)_2$ is present) (Cazalla et al. 2004); when the pH is below 9, the magenta is very pale; the phenolphthalein remains white or undyed in less alkaline and more neutral media in which $CaCO_3$ is more abundant.

Whenever possible, the binder and aggregates should be analysed separately. The acid method uses hydrochloric acid (8–10% HCl), which reacts with air-lime mortars and decomposes mainly calcitic compounds ($CaCO_3$) by causing effervescence (due to CO_2 release). This treatment is only suitable for air-lime mortars with silica aggregates. For mortars with carbonate aggregates, Casadio et al. (2005) assessed the efficacy of various separation methods, concluding that the use of ethylenediaminetetraacetic acid (EDTA) in concentrations between 0.1 M and 0.05 M is valid. Mechanical separation, although time-consuming, can also provide good results by determining at which point the fraction passing through a 150- μm mesh sieve can be considered binder. The mechanical component separation method guarantees the conservation of both components, whereas an attack with acids damages the binder, meaning it cannot be studied.

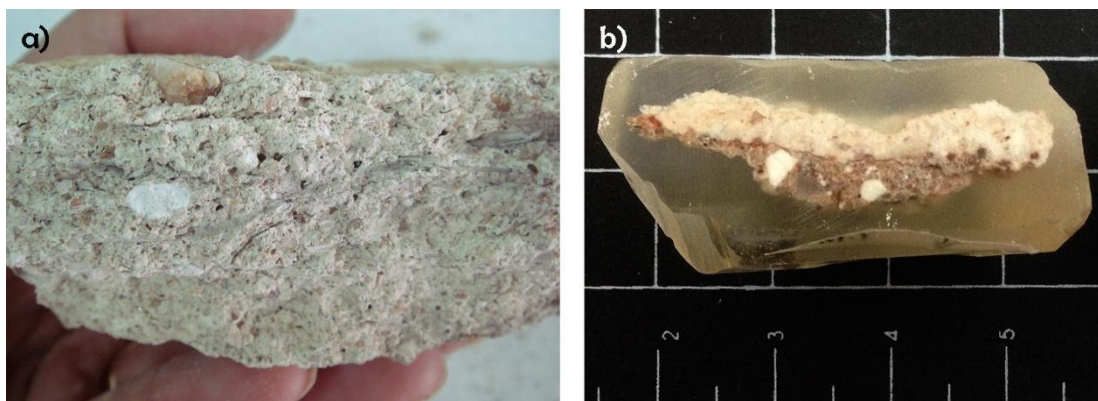


Figure 3. a) Example of an aerial lime plaster fragment (17th century) in which lime lumps (white) and plant remains (partially or totally decomposed; elongated shapes, dark-coloured) can be observed; b) Example of a two-layer plaster, light on top and dark on the bottom (17–18th centuries), encapsulated in resin due to its low cohesion, and ready to obtain thin sections for petrographic study.

3.1 Physical properties

1 Physical testing of mortars predominantly encompasses determination of pore structure. Due to the
2 porous nature of their binder, historic aerial mortars are soft materials with a density below 2.0 g/cm^3
3 ($1.5\text{--}1.8 \text{ g/cm}^3$) (Stefanidou 2010; Ergenç and Fort, 2019). One of the most frequent physical properties
4 analysed in building materials is **porosity** because of its significant role on core properties like strength
5 and durability. In general, the more extensive the mortars' carbonation process, the lower the porosity
6 and the higher the compressive strength (Schaffer et al 1993; Cazalla et al 2004). In addition to the
7 binder is the mortar compound, which accounts for most porosity, more than aggregates. In plasters,
8 porosity is usually lower than in bedding and pointing mortars (Pavia and Caro 2007).

9 The most appropriate techniques for measuring porosity in these mortars are as follows:

10
11
12
13
14
15
16
17 a) Porosity – and the different pore sizes and shapes, percentages, and types – can be characterized
18 using various microscopic techniques (stereomicroscopy, petrographic and scanning electron
19 microscopy, from low to high magnification). Image analysis techniques may also be used (Carò et al
20 2006; Stefanidou 2010) (see Section 3.3). Image analysis on photomicrographs permits 2D examination
21 of pores and the pore network using image-processing software, some of which is freely available (such
22 as ImageJ or JmicroVision). The data obtained can be also processed using software packages like
23 MATLAB.

24
25
26
27
28
29 b) Open porosity (accessible to water) and total porosity can be determined by vacuum-assisted water
30 absorption and hydrostatic weighing (in accordance with EN 1936:2007). Open porosity is defined as
31 the ratio (as a percentage) of the volume of the open pores to the apparent volume of the specimens,
32 while total porosity is the ratio (as a percentage) of the pore volume (open and closed) to the apparent
33 volume of the specimen. The standard, which is focused on natural stone, recommends the testing of
34 at least six specimens (cylindric, cubic or prismatic, with a minimum volume of 60 ml), requirements
35 that it is not always possible to fulfil in the field of cultural heritage. With this test it is also possible to
36 obtain the real and bulk densities of the mortar. The porosity of lime mortars from different historic
37 periods measured using this method ranges from 12 to 31% (Stefanidou 2010), 26 to 39 % (Ergenç and
38 Fort, 2019), and 29 to 44% (Ferreira Pinto et. al 2021).

39
40
41
42
43
44
45
46
47 c) Mercury intrusion porosimetry (MIP): This technique provides information such as porosity
48 accessible to mercury, pore size distribution, microporosity, apparent density, mean pore size, specific
49 surface and tortuosity in a pore diameter range between 0.001 and $400 \mu\text{m}$, depending on the
50 equipment. MIP is based on the fact that mercury is a liquid that does not wet solids. It consists of
51 intruding mercury at increasing pressure (usually from 1.4 kPa to 414 MPa) into the pore system of a
52 porous material. The volume of mercury intruded at low pressure relates to fine pores, while the
53 volume intruded at high pressure relates to large pores. Although the ASTM D4404 (2018) standard is
54 intended for soils and rocks, it can also be used for this test. In carbonated air-lime pastes, most pores
55
56
57
58
59
60
61
62
63
64
65

1 are reported to range between 0.4 μm and 1.0 μm (Arandigoyen et al 2005). When there is a
2 predominance of large pores – a characteristic feature of air-lime plasters – they will accommodate
3 the stresses induced by freeze-thaw and salt crystallization cycles (Ordoñez et al 1997; Stefanidou
4 2010). As it is a destructive test (samples are ultimately impregnated with mercury), representative
5 samples of the mortar type(s) should be selected for analysis. At least two samples (preferably prisms
6 of approximately 2 x 0.5 x 0.5 cm^3) should be analysed, although smaller and irregular-shaped samples
7 can be also measured. The toxicity and scarceness of mercury, combined with the associated
8 environmental issues, are some of the disadvantages of this technique. The results of this test have
9 been questioned due to the possible damage caused to the pores by the injection of mercury,
10 especially at high pressure.

11
12 d) Air permeability test: Gas permeability correlates with open porosity – the connected pores
13 available for fluid flow. Portable and non-destructive handheld air permeameters have become an
14 important analytical tool both in the laboratory and in situ (Filomena et al. 2014). The test is based on
15 the time that a specific volume of air takes to cross a specific volume of porous material. Measurement
16 using an air permeameter provides insights into the volume of pores with diameters of between 1 μm and
17 1 mm since there is a direct relation between air permeability and capillary absorption (Ergenç and Fort
18 2018). One of the main limitations of this technique is the need for standardized experimental
19 conditions.

20
21 e) Capillarity water test: Absorption by capillarity, which is a non-destructive test, provides information
22 about capillary porosity (EN 15801, 2009), which plays an important role in capillary rise in mortars (in
23 pore diameters ranging between 1 μm and 1 mm; Thomson et al 2004). The above-mentioned
24 standard determines the amount and rate at which a test specimen absorbs water by capillary action
25 through a test surface when in contact with water. It is recommended to test a minimum of 3 regular-
26 shaped specimens (i.e. cubes or cylinders with minimum dimensions of 10 mm per side or diameter
27 and a minimum height of 10 mm). In the specific case of mortars containing coarse aggregates, the
28 dimensions should be at least three times (and preferably five times) the size of the coarsest aggregate.
29 If anisotropy exists, the specimens should be orientated in the same direction. The parameters
30 obtained by this test are the capillary water absorption curve and coefficient, the height reached by
31 the capillary rising front and the capillary water penetration coefficient. Damas et al. (2018) show
32 capillary absorption coefficients ranging from 0.1 to 0.2 $\text{kg}\cdot\text{m}^{-2}\cdot\text{s}^{1/2}$ for aerial lime mortars from
33 buildings dating back to the 18th and 19th centuries. Magalhães and Veiga (2009) recorded similar
34 values (0.2 to 0.3 $\text{kg}\cdot\text{m}^{-2}\cdot\text{s}^{1/2}$) in historic mortars dating from between the 4th and 18th centuries in
35 Portugal, while Ferreira Pinto et al. (2021) reported values ranging from 0.2 to 0.6 $\text{kg}\cdot\text{m}^{-2}\cdot\text{s}^{1/2}$ in mortars
36 dating back to the 14th and 18th centuries, also in Portugal.

1
2
3
4
5
6
7
8
9
10
11
12
13
14
15
16
17
18
19
20
21
22
23
24
25
26
27
28
29
30
31
32
33
34
35
36
37
38
39
40
41
42
43
44
45
46
47
48
49
50
51
52
53
54
55
56
57
58
59
60
61
62
63
64
65

f) X-ray computed tomography (CT): This non-destructive method permits 2D and 3D high-resolution visualization of the internal structure of aerial mortars and plasters up to 4.5–16 μm , depending on the equipment. Total porosity (including open and closed pores) and pore size distribution are calculated from each CT scan (Divya Rani et al. 2021 refer to 100 CT scan slices in a mortar specimen of 10 x 10 x 10 mm; 3D reconstruction is then performed using image analysis techniques on all the CT scan slices); water movement can be followed as well (Bultreys et al 2016). Micro and nano CT systems, which have greater spatial resolution, have been increasingly used (Bugabi et al 2007; Sallam et al 2019; Rodriguez et al 2020). Because, in addition to the reasons above, they permit detection of very large or macropores and facilitate distinction between pores and fissures. Divya Rani et al (2021) analysed the porosity of ancient Indian lime mortars, recording 19% for a bedding mortar and 12% for a plaster sample. The main drawbacks of this method are its limited availability compared to other porosity analysis techniques (although availability has increased recently) and that it cannot detect the finest pores (nanopores).

All the porosity analysis techniques listed above – except for c) (MIP) – are non-destructive tests (provided that water, involved in some of them, does not interfere with mortar sample integrity), therefore allowing further analyses to be performed on the samples. For the techniques described in b), d), e) and f), when it is not possible to meet the size requirements set in the standards due to sampling limitations, three cubic mortar samples measuring 3–5 cm per side would be enough to perform all the tests.

Each of the techniques used to measure porosity encompasses different pore size intervals; the pores accessible from the outside are the most relevant for the weathering and fluid transport processes. Thomson et al (2004) and Divya Rani et al (2021) present extended studies about how to characterize the porosity of aged mortars. Historic aerial lime mortars have high porosity (> 20%) with a small volume of pores with diameters < 1 μm (Thomson et al. 2004). High-quality mortar shows a low volume of micropores and a small volume of larger pores (\leq 50 μm diameter) to prevent water absorption due to water vapour permeability (Barbero Barrera et al 2013).

The **colour** of mortars can be quantitatively measured using a spectrophotometer, a portable and non-destructive technique. Although there are various colour systems, the CIE L*a*b* one (International Commission on Illumination) is the most widely used in the cultural heritage field. The EN 15886:2010 standard details the testing techniques for colour measurement of surfaces. The standard describes the chromatic parameters to be measured (chroma, luminosity, hue and chromatic coordinates a* and b*) and the operating conditions (i.e. observer angle and illuminating reference) and specifies a minimum number of five specimens and a minimum of five readings for each of the specimens, when possible.

1
2
3
4
5
6
7
8
9
10
11
12
13
14
15
16
17
18
19
20
21
22
23
24
25
26
27
28
29
30
31
32
33
34
35
36
37
38
39
40
41
42
43
44
45
46
47
48
49
50
51
52
53
54
55
56
57
58
59
60
61
62
63
64
65

To measure the original colour of the mortar for both characterization and replacement purposes (not for partial or one-off restoration but for complete replacement of all the mortar), a non-exposed or inner surface should be selected. In the case of one-off restoration of a section or area of severely decayed mortar, the colour of the aged mortar surface should be selected so as to match the external chromatism as much as possible. The smoother the surfaces to measure, the better, as roughness affects chromatic values, especially the lightness parameter (L^*), which in the CIELAB space is dependent on the roughness of the surface (López et al 2018); therefore, the measured surfaces should show similar roughness. Whitish-cream Roman aerial lime mortars from Spain are reported to have high luminosity (70–85 units) and low chroma (saturation) (6–15 units) (Ergenç, 2017).

Ultrasound pulse velocity (UPV) testing is a portable and non-destructive technique used to measure the ultrasound propagation velocity of longitudinal or P waves (V_p), which can be used in air-lime mortars to check, mainly, their compactness (Cazalla et al 1999, 2004). The higher the compactness of the mortar, the higher the values of this velocity, based on the fact that ultrasound travels faster through solids than through gases (air contained in pores and fissures). In situ tests require indirect or surface mode measurement (both transducers – ultrasound emitter and transmitter – are placed on the same plane), while in laboratory measurements direct transmission can be used (transducers are placed in parallel and on opposite planes of a cubic or prismatic mortar specimen) and anisotropy indices can be calculated (difference between the values obtained when measuring along each of the three spatial axes). According to Cazalla (2000), the total anisotropy index (ΔM , Guyader and Denis 1986) accounts for variations due to changes in porosity and compaction, among others, while relative anisotropy (Δm) results from variations in the compaction plane. The lowest V_p values usually correspond to the direction perpendicular to the compaction of the mortar (applicable to both bedding and pointing mortars, and plasters). To ensure the best contact between the transducers and the mortar surface, and to minimize the effect of surface roughness on the measurement, it is advisable to use a plastic membrane.

With UPV measurement, especially when ultrasound S or transverse waves are used, it is possible to calculate the elasticity modulus of the mortars, which identifies the deformation capacity of a material under stress (Tunçoku and Caner-Saltık 2006; Güney 2012). Historic aerial lime mortars dating back to the 12th and 13th centuries show an elasticity modulus of 1–3 GPa (Tunçoku and Caner-Saltık 2006).

3.1.1 *Hydric properties*

Water movement and hydric properties can be determined by the following tests:

- water absorption at atmospheric pressure (as a percentage), in accordance with EN 13755 (2008). The specimen, once dried and after recording its weight, is completely immersed in water (keeping a 25-mm layer of water over its top surface) until it acquires a constant weight

(its weight is recorded every 24 hours). The standard, which is intended for natural stone, recommends measuring a minimum of 6 specimens of geometric shape (cubes, prisms or cylinders) of about 50–70 mm per side or diameter.

- water absorption by capillarity, in accordance with EN 15801 (2009), already described in Section 3.1.e. There is also another standard (EN 1015-18, 2002) for determining the water absorption coefficient due to capillary action of hardened mortar for masonry, although it is intended for fresh mortars (including aerial lime mortars).
- water absorption by the pipe method (EN 16302, 2013): The purpose of this test is to measure the penetration of water into the material under a pressure analogous to that exerted by rainwater. The method can be used both in the laboratory and in situ due to its non-destructive nature (and on both vertical and horizontal surfaces), and consists of determining the amount of water (ml) transferred from the pipette (or Karsten tube) through a given test area (cm²) over a set time, expressed in ml/cm². At least three specimens or mortar surfaces (for each type of mortar) should be measured, and for mortars containing coarse aggregates the area diameter to be measured should be at least three times (and preferably five times) the size of the coarsest aggregate. If anisotropy exists, the specimens should be orientated in the same direction. The Karsten tube must be firmly fixed to the measuring surface (which must be smooth and without visible cracks) by mechanical methods or by using a suitable removable sealing material to avoid water leakage.
- water vapour permeability, in accordance with EN 15803 (2009). In this test, penetration of water vapour through the thickness of a specimen is measured by subjecting the specimen to different partial water vapour pressures (reached using the different saturated saline solutions and gels proposed by the standard). The standard recommends two possible types of cuvette or device for the test, with the dimensions of the three specimens (the minimum number recommended) depending on this choice. If anisotropy exists, the specimens should be orientated in the same direction. Maximum specimen thickness should be 20 mm; in the case of mortars with coarse aggregates, it should be at least twice the size of the coarsest aggregate.

Not only are these water absorption tests of interest when studying these mortars, it is also of interest to examine how the absorbed water evaporates during the drying stage (EN 16322, 2013). The drying properties of materials can be calculated from a curve indicating the weight loss of the mass of water inside the test tube (previously saturated with water), as a function of time, during a drying experiment. The number of specimens, the dimensions and the orientation in the event of anisotropy are the same as described in Section 3.1.e (capillary water test).

1
2
3
4
5
6
7
8
9
10
11
12
13
14
15
16
17
18
19
20
21
22
23
24
25
26
27
28
29
30
31
32
33
34
35
36
37
38
39
40
41
42
43
44
45
46
47
48
49
50
51
52
53
54
55
56
57
58
59
60
61
62
63
64
65

In the case of low cohesion of the mortar samples, it is not advisable to carry out tests in which water is involved, which may lead to crumbling of the mortar, as well as producing erroneous results. Arizzi and Cultrone (2014) suggest considering the possible alteration of mortar microstructure due to reactions with water when interpreting the hydric behaviour of mortars, although this occurs mainly in fresh mortars.

3.2 Mechanical properties

Analysing the mechanical properties of mortars is crucial for evaluating the structural performance of historic masonry since raw material characteristics and lime mortar production technologies contribute to variability in structural conditions and composition. The reaction products in the matrix and the integration of the newly formed crystals are what give mortar its mechanical strength. The microstructure (i.e. the size, shape and orientation of the crystal phases) of the binder essentially determines the engineering properties of the material.

Mechanical testing includes measuring the strength characteristics of the mortar (compression, tensile and shear strength, EN 1015-11: 2019), the elasticity modulus, and the adhesive strength of hardened rendering and plastering mortars on substrates (EN 1015-12: 2016). Both standards refer to the testing of moulded mortars.

These characteristics cannot always be measured directly due to difficulties in obtaining sufficient material volume for some of the standardized tests (compression and flexural tests, adhesive strength; due to their destructive nature they are more appropriate when designing new air-lime mortars for replacement, which is not the focus of this TC chapter). Velosa et al. (2010) emphasize the difficulty of working with archaeological mortar samples because of their insufficient amounts and irregular shapes. Therefore, mechanical and physical tests cannot be conducted using engineering standards.

Air-lime mortars show compression strengths of between 1.5 and 2.5 MPa and are therefore used in building applications that do not provide a support function (Stefanidou 2010; Ferreira Pinto et al. 2021). Dolomitic lime is reported to exhibit more shrinkage and lower carbonation, resulting in lesser mechanical properties (Arizzi and Cultrone 2012).

Some authors employed the point-load test to measure the compression strength of small (> 25 mm thickness) fragments of ancient lime mortars (Tuñçoku and Caner-Saltık 2006; Güney 2012). Drdáccký and Slížková (2007) describe non-standard tests for small samples of historic mortars that allow them to study the mechanical strength of these materials.

The strength of an aerial lime mortar is proportional to the strength of the weakest component – the binder – in our case aerial lime (Lawrence 2006).

1 A **DRMS (drilling resistance measurement system)**, a minimally destructive technique) measures the
2 resistance offered by a material when drilled. It is therefore possible to measure changes in this
3 resistance from the surface to the interior of the mortar, either through mortars or across plasters
4 (Rodrigues et al 2002). The force that is required to drill an orifice (a few millimetres in diameter,
5 depending on the drill bit) under specific operating conditions correlates to the compressive strength
6 of the measured material (and with ultrasound velocity according to Costa et al 2012). Nevertheless,
7 the heterogeneity of mortars deriving from their characteristic granular texture (binder and
8 aggregates) sometimes produces very irregular drilling curves that are hard to interpret, especially in
9 aerial lime mortars with siliceous aggregates due to the strong contrast between the
10 hardness/resistance of the soft lime-based pastes and the siliceous particles of the aggregates (Ferreira
11 Pinto et al. 2021). A minimum of 3–5 drillings is recommended, although more drillings should be
12 performed when the results obtained are too widely dispersed.
13
14
15
16
17
18
19
20
21
22
23

24 Aerial lime mortar **hardness** can be measured using the rebound hardness test (Pinto et al 2012).
25 Today, these measurements can be taken with portable and non-destructive equipment (Ergenç and
26 Fort 2018; Ergenç et al 2018a) thanks to recently developed low-impact surface hardness testers such
27 as Equotip by Proceq (Wilhelm et al. 2016), a device as small as a pen (and with the shape and
28 appearance of one). The contact diameter of the probe (inside which is the metal sphere that impacts
29 the surface) is 0.5 mm. This means that the area of the mortar surface to be measured has to be known
30 in advance, indicating when we are measuring an aggregate (or an area enriched in aggregates) or
31 binder. This, together with the rough surface of mortars, and the significant difference in the case of
32 siliceous aggregates in contrast to lime paste, can result in low reading repeatability, which has to be
33 balanced with a high number of measurements (starting with a minimum of 5–10 readings). In general,
34 hardness values measured on the external surface of aerial lime mortars are higher than those taken
35 inside, given that carbonation is usually completed in the external areas and may not be so in the
36 internal ones (Lawrence 2006). Roman aerial lime mortars are reported to have surface hardness
37 values of between 170 and 442 LH (Leebs Hardness) (Ergenç, 2017).
38
39
40
41
42
43
44
45
46
47
48
49
50
51
52

53 **3.3 Petrographic characterization**

54 Petrographic analysis provides valuable information on the technology of manufacturing lime and its
55 mortars, as well as on their composition, texture and state of development and conservation (Hughes
56
57
58
59
60
61
62
63
64
65

1 and Cuthbert 2000; Pavia and Caro 2006, 2007, 2008; Elsen 2006; Karkanis 2007; Ergenç, 2017;
2 Balksten et al 2019). It is a destructive technique that needs a sample size larger than 1 cm³.

3
4 Although there are different types of microscopes, petrographic microscopes (polarizing light optical
5 microscope) have been the most widely used in Europe to study lime mortars since the 1970s due to
6 their accessibility and high efficiency (Elsen 2006; Balksten et al 2019). The different microscopic
7 techniques for characterizing aerial lime mortars are described below.
8
9

10 11 12 13 **3.3.1 Stereomicroscopy**

14 Stereomicroscopy allows detailed macro-observation – complementary to naked-eye observation – of
15 aerial lime mortar samples, specifically the distribution, morphology and size of the aggregates, pore
16 shape and size, the presence of fissures and cracks, as well as of contact between layers, if present,
17 and between mortar and substrates. A rough estimation of the binder/aggregate ratio can be obtained
18 with this technique. Portable and handheld digital microscopes (e.g. Dino-Lite) with up to 900x
19 magnification, 5-megapixel resolution and specific illumination – such as ultraviolet or infrared – are
20 now commercially available.
21
22
23
24
25
26
27
28

29 **3.3.2 Polarized optical microscopy**

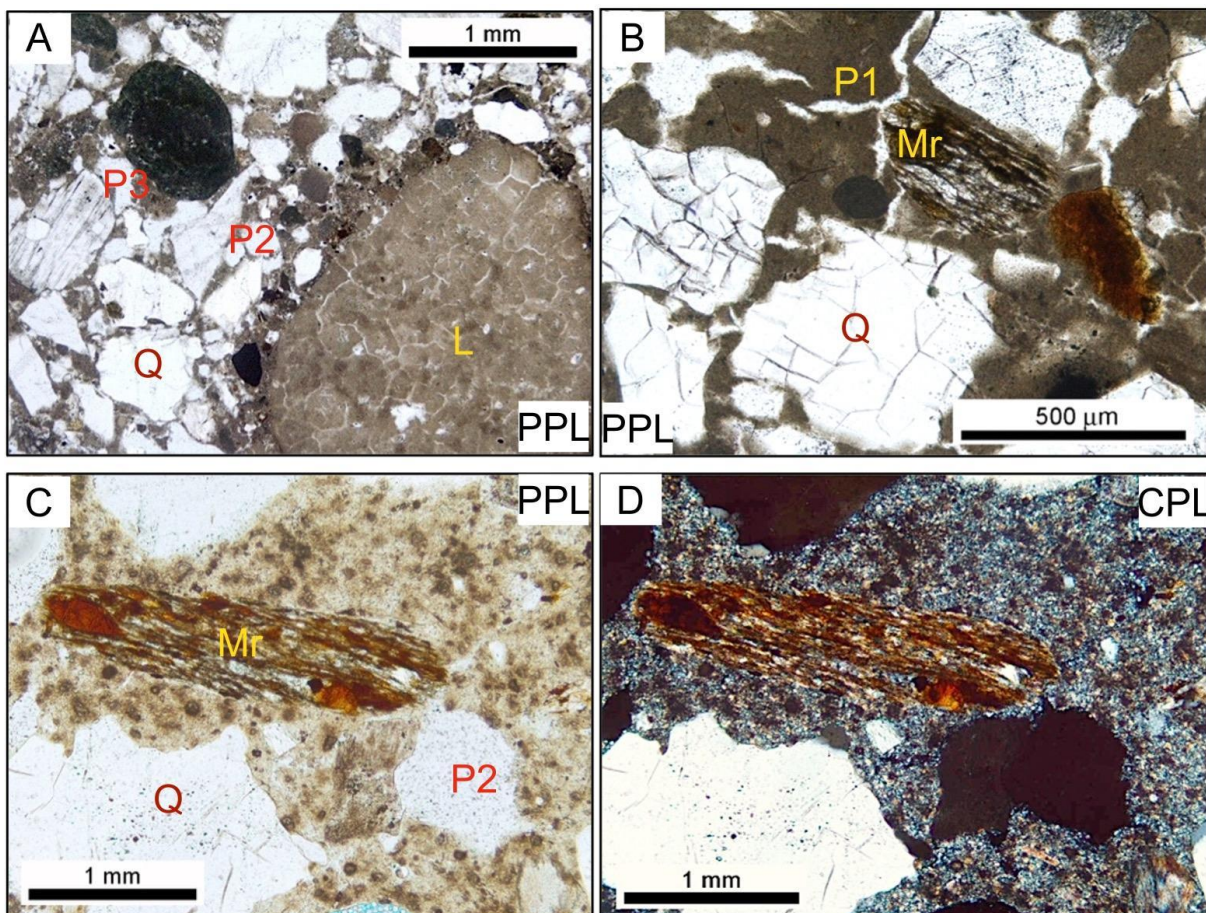
30 Petrographic microscopy (and, specifically, transmitted polarized light optical microscopy-POM;
31 reflected light optical microscopy permits identification of pigments in mortars in accordance with EN
32 17187:2020) is considered the most useful analytical tool for studying the mineralogy and texture of
33 mortars (Barnett 1991; Goren and Goldberg 1991; Lindqvist and Sandström 2000; Hughes and
34 Cuthbert 2000; Affonso and Freiberg 2001; Hughes et al 2001; Degryse et al 2002; Elsen 2006;
35 Middendorf et al 2005; Karkanis 2007; Blaeuer and Kueng 2007; Pavia and Caro 2008; Balksten et al
36 2019). It also provides information about the complexity of the chemical and physical changes in the
37 mortars during setting and carbonation (hardening and curing). It is likewise a useful tool in the
38 diagnosis of degradation of historic mortars (Elsen 2006; Pavia and Caro 2007).
39
40
41
42
43
44
45
46
47

48 For the petrographic study, thin sections of mortar samples must be prepared. Preferably, these
49 sections will be cut perpendicular to the external surface of the mortar to obtain the whole picture
50 and the variation from the surface to the interior. If soluble salts are present, production of the thin
51 sections will use oil instead of water. Frequently, the loss of cohesion in historic aerial lime mortars
52 makes it necessary to encapsulate them in resin beforehand to prevent them crumbling when
53 obtaining the thin sections (Figure 3b). Once the resin has hardened, the mortar sample can be cut
54 into 5-mm-thick slices; the most common thin-section area is 3 x 2 cm². This mortar slice is glued to a
55
56
57
58
59
60
61
62
63
64
65

1
2
3
4
5
6
7
8
9
10
11
12
13
14
15
16
17
18
19
20
21
22
23
24
25
26
27
28
29
30
31
32
33
34
35
36
37
38
39
40
41
42
43
44
45
46
47
48
49
50
51
52
53
54
55
56
57
58
59
60
61
62
63
64
65

glass sample holder on one side, and the other side is ground down into a standard 30- μm -thick (0.03 mm) thin section; this is the necessary thickness to observe the optical properties of minerals. The thin sections can be protected with lacquer or a coverslip. They are then labelled and are ready to be examined under the polarizing microscope. Goren (2014) describes the process in detail, using a portable petrographic thin-section laboratory for microscopic analysis of archaeological artifacts. The technique for the preparation of thin sections and for petrographic description is included in the EN 12407:2019 and EN 17187:2020 standards. Although the technique is destructive, for a thin section only a small centimetre-size sample is required.

Staining techniques can be applied to thin sections to highlight and differentiate between various minerals. Red alizarin is one of the dyes most widely used to stain lime mortars to differentiate between carbonates (calcite versus dolomite): calcite stains red while dolomite either does not stain, or stains blue if it contains Fe^{2+} (Dickson 1966).



1
2
3
4
5
6
7
8
9
10
11
12
13
14
15
16
17
18
19
20
21
22
23
24
25
26
27
28
29
30
31
32
33
34
35
36
37
38
39
40
41
42
43
44
45
46
47
48
49
50
51
52
53
54
55
56
57
58
59
60
61
62
63
64
65

Figure 4. POM images of aerial lime mortars in parallel (PPL) or cross-polarized (CPL) light mode. A-B-C. Mortars in PPL with a brown cryptocrystalline binder and siliceous aggregate (Q-quartz and/or Mr-metamorphic rock fragments). A. Mortar with abundant vascular porosity (semi-circular, P2) and irregular (P3), many aggregates, not much binder and lime lumps (L) that may contain fissural porosity. B. Mortar with abundant fissural porosity (P1) and highly fractured quartz aggregate. C. Appearance of the binder in PPL during its carbonation process. D. The birefringence of the binder (CPL) indicates its degree of carbonation (portlandite-grey to black and calcite-dark brownish).

Analysis of thin sections of aerial mortars can provide answers to a wide variety of questions. The method requires experience and expertise from both the technician who prepares the thin sections and, especially, from the analyst (the petrographer), often a trained specialist. There are many petrographic atlases, which are excellent tools for identifying the different components of these mortars under the microscope (Blaeuer and Kueng 2007; Ingham 2011; Pecchioni et al 2013; EN 17187:2020).

The study focuses on distinguishing the components of the mortar (Figures 4 and 5) (Elsen 2006; Pavia and Caro 2007; Balksten et al 2019):

- **Lime binder.** The petrographic study can identify the provenance of the carbonate rock (raw material-limestones, dolostones), degree of calcination, slaking and hardening, as well as the presence of fragments of incompletely calcined limestone and of lime lumps (Hughes and Cuthbert 2000; Pavia and Caro 2008). It is also possible to determine the calcitic or dolomitic nature of the binder since dolomite does not stain red. In POM, the binder of an aerial lime mortar is seen as a cryptocrystalline mass (crystal size < 4 μm) of dark brown or green colour (PPL; Figures 4A-C and 5), highly similar to the so-called micritic limestones of sedimentary origin, from which the binder may have come (Goren and Goldberg 1991; Leslie and Hughes 2002; Karkanas 2007). The binder may show processes of dissolution and dissolution-recrystallization, recognizable by analysing the grading of the binder crystal sizes and shapes. It is also possible to establish the degree of carbonation reached by the binder, considering the transition of textures (the texture being the set of intergranular or intercrystalline spatial relationships and morphological characteristics – size and shape – of the mortar components), which can be detected using POM and that is related to both the degree of crystallinity and the degree of birefringence (an optical property of minerals related to interference phenomena of polarized light with anisotropic media) of these crystalline masses (Karkanas 2007; Balksten 2019). The greater the presence of calcite (calcium carbonate, CaCO_3) versus portlandite (calcium hydroxide, $\text{Ca}(\text{OH})_2$), the more extensive the carbonation process achieved by these mortars. In POM, hydrated or slaked lime

1 (portlandite, CaOH_2) is poorly crystallized, showing a lower degree of birefringence than calcite
2 (calcium carbonate, CaCO_3), which is better crystallized and shows medium birefringence (Figures 4C-
3 D). On many occasions, to determine the shape of these microcrystals it is necessary to use scanning
4 electron microscopy (SEM), as this technique offers higher magnification and resolution (Elsen 2006).
5 An optical light microscope with a 50x objective lens allows relatively good observation down to crystal
6 or grain sizes of 50–60 μm .
7

8
9
10 In aerial lime mortars it is very common to find lime nodules (lime lumps) of different sizes (Figures 3a,
11 4A, 5B, 5D-E and 5G-H). Up to 35% lime lumps (ranging in size from 50 μm to 10 mm) can be found in
12 the binders of historic mortars (Leslie and Hughes 2002, Ingham 2011). Poorly burnt limestone
13 fragments preserve internal geological features characteristic of the original limestones (e.g. fossils or
14 sedimentary structures). These fragments are formed either because the kiln did not reach the
15 calcination temperature (800 °C) or because of the location of these fragments in the kiln, in which
16 heat distribution was uneven. These lime lumps may also be a result of poor slaking of quicklime or
17 poor mixing of the mortar components, thus providing information about the techniques used to
18 produce these mortars in different historical periods in a region (Affonso 1996; Hughes et al 2001;
19 Karkanis 2007; Pavia and Caro 2007; Balksten et al 2019). These lime lumps can be identified under a
20 microscope as follows:
21
22

- 23 1. When they have explicit boundaries, it can be inferred that they are uncalcined limestone
24 (Figure 5B).
- 25 2. When they show poorly defined boundaries, it implies a lack of slaking water during mortar
26 manufacture (Figures 5D-E).
- 27 3. Their shape enables identification and separation, since lime nodules are more rounded
28 (Figures 4A and 5G-H) than poorly burnt limestone fragments (Figure 5B) and their internal
29 composition is more homogeneous (lime lumps have fewer coloured halos due to calcination).
30

31
32
33
34
35
36
37
38
39
40
41
42
43
44 - **Aggregate:** Historically, aggregates were cleaned of salts and clays both so that they would adhere
45 well to the lime binder and to prevent decohesion. The nature of the aggregates can vary: a) natural
46 (silicates and/or carbonates), depending on the regional geology surrounding the location of the
47 mortars, or b) artificial (ceramics, recycled material from other building works) (Figures 4 and 5;
48 Ingham 2010). Among the silicates, quartz, feldspar and mica are the most abundant minerals and can
49 appear as isolated grains or as part of rock fragments (igneous, metamorphic and/or sedimentary
50 polymineral grains; e.g. granite, basalt, shale, slate, sandstone). According to EN 17187 (2020),
51 aggregates are divided into reactive or hydraulic (crushed ceramics or volcanic rocks – pozzolans and
52 ashes), and inert or non-reactive (other rocks and geological sediments, excluding volcanic and other
53
54
55
56
57
58
59
60
61
62
63
64
65

1 recycled artificial materials). It should also be noted that the shape (angular or rounded) of the
2 aggregate grains indicates whether the aggregate was extracted directly from the banks of a river
3 (rounded or sub-rounded shapes) or whether it comes from the crushing of quarried or artificial stone
4 (angular shapes) (Bustillo-Revuelta et al. 2014) (Figures 3, 4 and 5, Fort et al. 2004). The presence of
5 rounded and poorly sorted aggregates (from 0.063 mm to 4 mm) facilitates the workability of the
6 mortars (Ingham, 2011). In historic plasters, it is common to find well sorted and sub-angular
7 aggregates that can reduce drying shrinkage problems (Ingham, 2011). The high reactivity of the lime
8 and its high adhesion to the aggregate results in unclear contacts between the two components
9 (Figures 4 and 5; Leslie and Hughes, 2002; Elsen, 2006; Pavía and Caro, 2008; Rafanelli et al. 2017;
10 Gliozzo et al. 2021, this TC).

11
12
13
14
15
16
17
18 - **Pores:** The morphology, size, distribution, quantity and structure of the pores can be measured in
19 thin sections. These data can provide information about the manufacturing process of these mortars.
20 The porosity of these mortars mainly affects the binder (Figures 4 and 5). The following types of pores
21 are frequent in aerial lime mortars (Hughes and Cuthbert 2000; Leslie and Hughes 2002; Elsen 2006):

22
23
24
25 a) Rounded or sub-rounded pores (vascular pores), which are produced by the techniques used to
26 manufacture and/or place the mortars on site, where fluids – entrained or entrapped air – are trapped
27 in the mixture (Balksten et al 2019).

28
29
30
31 b) Fissures and cracks, which appear frequently both in the binder and inside the lime lumps, and/or
32 in the binder-aggregate contact in these mortars. They are due to shrinkage of the aerial lime during
33 setting and carbonation (Affonso 1996; Leslie and Hughes 2002; Karkanis 2007; Pavia and Caro 2007,
34 2008). They may also be due to the presence of salts and clays, mainly related to the edges of the
35 aggregates.

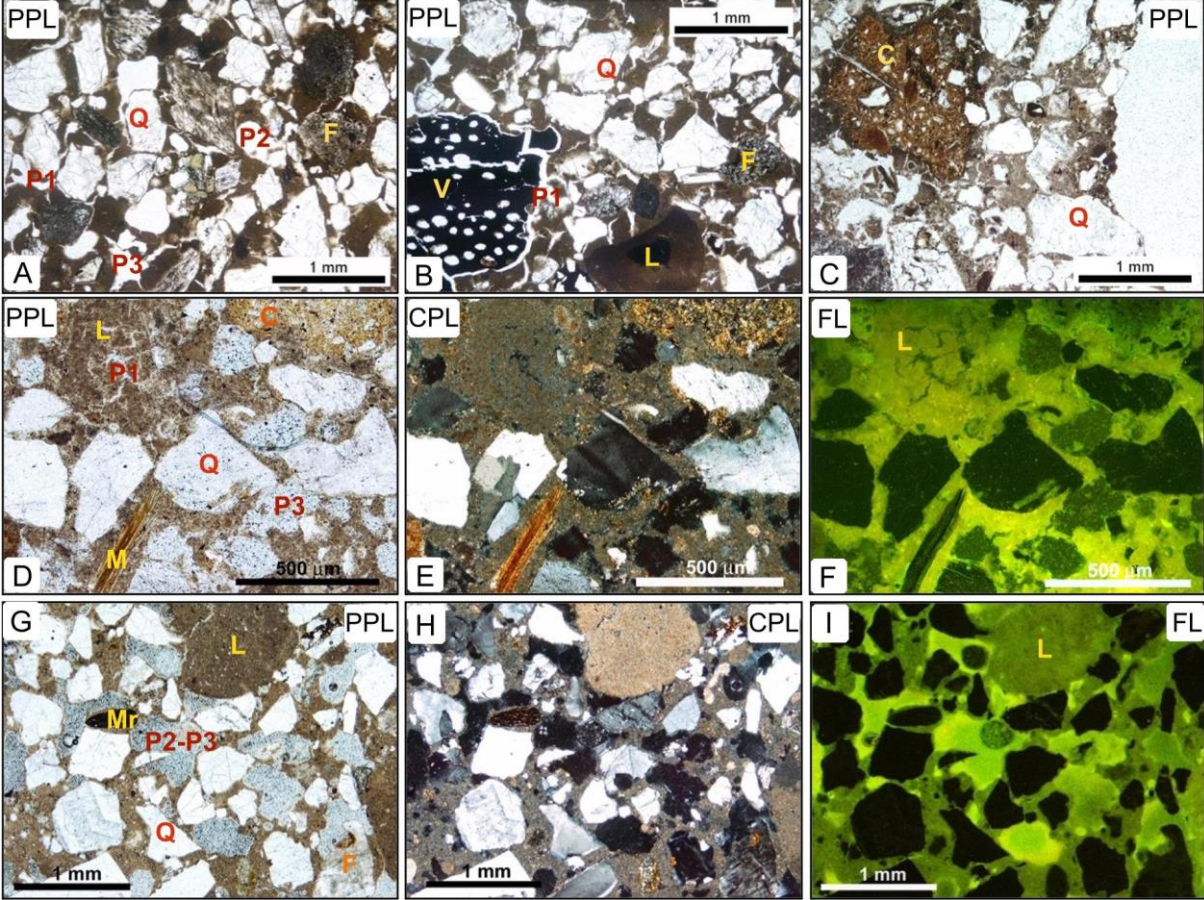
36
37
38
39
40
41 c) Irregular or secondary porosity (frequently composed of irregular-shaped pores), which mainly
42 affects the binder and is due to post-carbonation dissolution processes related to changes in and
43 degradation of the mortar (Elsen 2006; Pecchioni et al 2013). Subsequent recrystallization at pore
44 margins leads to angular and lenticular pores becoming rounded (Leslie and Hughes 2002). This filling
45 of some fine cracks and capillary pores by recrystallization of calcite, the so-called “self-healing”
46 capacity of lime mortars, increases the mortars’ durability (Lubelli et al 2011).

47
48
49
50
51
52
53
54 - **Binder/aggregate relationship:** By estimating the binder/aggregate ratio it is possible to indicate the
55 proportion of binder and aggregates used to manufacture these mortars. The ratio is usually given in
56 volume. A very rough visual estimation can be made by manually counting points under the
57 microscope. Recently, it can be made by using image-processing tools (Carò et al 2006). The contact
58
59
60
61
62
63
64
65

1 between binder and aggregates can also be analysed, especially in terms of degree of
2 adhesion/bonding of the two mortar components, fissured contacts, or the existence of crystal
3 neoformation (recrystallization processes) in between them.
4

5 The binder/aggregate ratio and the percentage, average size and distribution of both aggregate and
6 pores and fissures can be determined using image-processing software (Elsen 2006; Pavia and Caro
7 2007, 2008; EN 17187:2020).
8
9

10
11 - **Additives/admixtures:** Compounds added to the mortars to enhance specific properties such as
12 strength, waterproofing, aesthetics and durability can be distinguished by petrographic analysis.
13 Organic additives include charcoal particles (which could also be a result of kiln contamination) and
14 plant fibres and remains (Figures 3A and 5B). Carbonaceous compounds are observed as irregular
15 grains, of variable size, which may appear with fissures in their perimeter. Plant remains may be whole
16 or partially/completely decomposed. In the former case their cell structure is well defined, and in the
17 latter they leave the shape of their moulds as pores. Inorganic additives like ceramic fragments,
18 volcanic ash, furnace slag or ferric compounds may also exist (EN 17187:2020) (Figure 5C).
19
20
21
22
23
24
25
26
27



1
2
3
4
5
6
7
8
9
10
11
12
13
14
15
16
17
18
19
20
21
22
23
24
25
26
27
28
29
30
31
32
33
34
35
36
37
38
39
40
41
42
43
44
45
46
47
48
49
50
51
52
53
54
55
56
57
58
59
60
61
62
63
64
65

Figure 5. POM images of historic aerial lime mortars (17th century), in parallel (PPL) or cross-polarized (CPL) light mode. A to I. Siliceous aggregates can be very abundant (Q: quartz; F: feldspar; M: mica; Mr: metamorphic rock fragments), along with different types of lime lumps (L). Porosities – fissural (P1), circular-vacuolar (P2) and irregular (P3) – abound in the dark microcrystalline binder. B, C and D. There may be organic inert additives (V) and/or inorganic (ceramic fragments, C) additives. E and H. The average birefringence of the binder (CPL) indicates its degree of carbonation. F and I. Fluorescence microscope images (FL), where the green intensity reflects the degree of porosity, which affects the binder and the lime lumps.

3.3.3 Scanning electron microscopy

Due to its higher resolution (up to 10,000x magnification), SEM is the other significant step in the process of microscopically characterizing lime mortars (Gourdin and Kingery 1975; Kingery et al 1988, 1991; Elsen 2006; Karkanis 2007). SEM analyses can be performed on mortar fragments (< 1 cm³) or on thin polished sections (the same thin sections previously prepared for POM can be used, but without any lacquer or coverslip). A scanning electron microscope equipped with an EDS (energy-dispersive X-ray microanalysis device) and SE (secondary electron) and BSE (back-scattered electron) detectors provides significant qualitative and semi-quantitative information about crystal morphology and the chemical composition of the binders and lime lumps, as well as size measurements of crystals and grains (for quantitative analysis, use of an electron microprobe is required, which is much more expensive and time-consuming, but much more accurate) (Figure 6). It also offers the possibility of element mapping and of obtaining information about the changes in lime binders while they are carbonating (Randonjic et al. 2001; Cultrone et al. 2005; Elsen 2006; Stukovnik et al. 2016; Ergenç et al. 2018b). It likewise allows further study of recrystallization and dissolution processes within the binders. Study of the aggregates using SEM-EDS complements and deepens the analysis (which must be carried out previously using POM, especially in the case of ceramic aggregates or aggregates recycled from other artificial materials, or even from other mortars), or when differentiating between the various types of feldspar (microcline, albite, etc.) or determining the nature of rock fragments.

SEM analysis requires the metal sputtering of the sample to be electron-conductive; environmental scanning electron microscopy (ESEM) does not require this prior step, and samples can be used for other analyses as the technique is non-destructive.

The data and images obtained can be digitally processed using the same image-processing and statistical software used in POM in order to confirm, complete and improve the same types of information (binder/aggregate ratio; percentage, average size and distribution of both aggregate and pores, etc.).

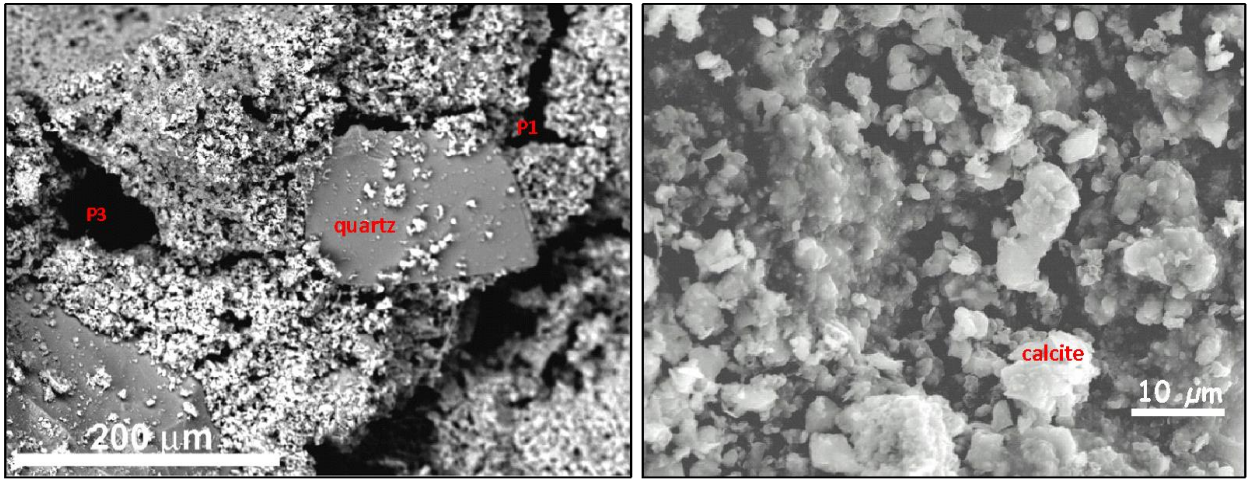


Figure 6. SEM images in BSE mode of an aerial lime mortar fragment from the 17th century. Pores can be observed as irregular (P3) and fissural (P1), which affect the binder of these mortars and the edges of the siliceous aggregates. The degree of crystallinity of the binder improves with its carbonation, forming well defined crystals (calcite - CaCO₃; white crystalline aggregates).

1. 3.3.4. Other microscopy techniques

Fluorescence microscopy (FM) combines the use of POM with fluorescence microscopy (Figures 5D-I). FM can be described as POM to which an illumination source that emits ultraviolet light has been coupled. Fluorescence is the property of some organic or inorganic compounds to absorb ultraviolet light and partially re-emit it. Therefore, mortar samples that are to be analysed using FM but that are not naturally fluorescent need to be impregnated with a fluorescent substance (fluorescein). This is added to a resin that is then inserted into the sample during thin-section preparation (Varas-Muriel 2012). The FM method is suitable for identifying both inorganic and organic components, and also for examining the porosity of mortar (Elsen 2006; Pavia and Caro 2007; Ingham 2011; Balksten et al. 2019). Organic compounds show a certain natural fluorescence when irradiated with ultraviolet light, which is especially of interest in detecting the presence of organic additives. On the one hand, the fluorescein substance incorporated in the resins used to make the thin sections of these mortars stains the most porous areas a very intense green when ultraviolet light is reflected on them (Figures 5F and 5I). It can also be seen that the binder itself and its lime lumps have a certain fluorescent mottling due to their internal microporosity (Figures 5F and 5I). On the other hand, the grains that constitute the aggregate, when dense, with no pores or fissures, remain black, without any fluorescence. Using this technique, the distribution, size and quantity of aggregates and of existing pores and fissures in any component of the mortars can be calculated with the help of image analysis software (Pavia and Caro 2007; Ingham 2011).

1
2
3
4
5
6
7
8
9
10
11
12
13
14
15
16
17
18
19
20
21
22
23
24
25
26
27
28
29
30
31
32
33
34
35
36
37
38
39
40
41
42
43
44
45
46
47
48
49
50
51
52
53
54
55
56
57
58
59
60
61
62
63
64
65

Cathodoluminescence coupled to a polarized optical microscope (POM-CL) allows the identification of the components and geological/mineralogical transformation processes that carbonate rocks have undergone (Walkden and Berry 1982; Machel 2000; Chapoulie et al. 2005). This technique uses the same thin section as POM, but not the one used in FM, as in the latter an impregnating fluorescent substance is required. These components emit luminescences of different wavelengths when irradiated with an electron beam. The ability to differentiate between different carbonate phases (or carbonate of different origins) is the reason for using this technique to study historic mortars, as it makes it possible to differentiate calcium carbonate (CaCO_3) of geological/natural origin (original grains) from that generated by the pyrogenic process (Elsen 2006; Lindroos et al 2007; Michalkska and Czernik 2015; Hayen et al 2016), namely replacement calcite (or calcite recrystallized after mortar setting) (Hiatt and Pufahl 2015) or calcium carbonate formed by calcium hydroxide carbonation. The use of POM-CL therefore makes it possible to assign a fragment composed of calcite to a natural aggregate or to a neo-formed crystal due to dissolution-precipitation processes.

Cathodoluminescence coupled to a scanning electron microscope (SEM-CL) allows resolutions at a micrometric level and, above all, allows intensity and wavelength values to be obtained for each point (not possible with POM-CL), with the possibility of mapping the wavelengths emitted by the mortar components in the range between 300 and 900 nm (Toffolo et al 2020). Under this technique, CaCO_3 of geological origin emits at about 620 nm, resulting in orange tones, while the carbonated lime mortar binder emits at 450 nm, producing a blue tone (Toffolo et al 2019).

Lime lumps can also be differentiated by their luminescent areas, which are usually orange-red; dark red to purple colours are observed in under-burnt limestone fragments (Lindroos 2005; Lindroos et al 2007; Murakami et al 2013, Lindroos et al 2014).

2. 3.4. Mineralogical characterization using X-ray diffraction

X-ray diffraction (XRD) permits identification of the different minerals in aerial mortars and plasters (Elsen 2006; Balksten et al 2019). One of the main disadvantages is that there are minerals in these mortars that overlap and are masked in the diffractograms, with some of them sharing XRD peaks, making it difficult to identify each of them (Igea et al 2012; Jordan et al 2019). To analyse samples using this technique, approximately 2 g of sample (depending on the equipment) is required. This has to be ground to a powder with a particle size of $< 53 \mu\text{m}$. After analysis, the sample can be used in other analyses.

Historic aerial lime mortars contain a number of characteristic minerals: calcite (the main component of both the carbonated binder and/or the carbonate aggregate), and quartz (common component of the siliceous aggregate). This simple mineralogy can get more complex when the lime is dolomitic (we

1 will find dolomite), the aggregates are not only quartz (feldspars, micas, rock fragments), and
2 subsequent alteration products are added (saline compounds such as gypsum) (Alvarez et al 2000;
3 Biscontin et al 2002; Mota-López et al 2016).

4
5 This analytical technique can only detect mineral phases present in more than 4% wt. If the hydraulic
6 phases are below this amount, they cannot be detected. For this reason, to determine whether the
7 mortar is hydraulic or aerial, the binder is also analysed by separating the aggregate, if possible.
8
9 Nevertheless, in most historic mortars, physical separation of their different components is difficult to
10 achieve without damaging them or causing any of them to disappear. It is therefore highly common to
11 carry out the mineralogical study on the powder fraction of the whole sample. When this happens,
12 prior microscopic analysis is mandatory to assign the obtained mineralogy to each of the mortar
13 components. Figure 7 shows an example of XRD analysis of a historic aerial lime mortar with siliceous
14 aggregates. Identification of carbonate minerals is as follows: main calcite peak at 3.03 Å; main
15 dolomite peak at 2.88 Å. These two minerals are associated with the binder and/or the carbonate
16 aggregate, the presence of the latter having to be previously confirmed by POM. The presence of
17 portlandite (main hydrated lime peak at 2.63 Å) is associated with incomplete carbonation of the lime
18 binder. The siliceous minerals identified (quartz 3.34 Å, feldspars 3.24–3.18 Å and micas 10–9.9 Å,
19 mainly) can be considered as part of the aggregate, which may appear as grains composed of a single
20 mineral (e.g. quartz, feldspars or micas) or as rock fragments – composed of more than one mineral –
21 of different origins (sedimentary, igneous and/or metamorphic; e.g. granite is composed mainly of
22 quartz, feldspars and micas). Rock fragments, which are so useful for provenance studies, must be
23 studied using POM. Organic compounds (e.g. additives) cannot be detected by this technique, as they
24 do not constitute crystalline phases. The absence in the binder of minerals such as wollastonite,
25 gehlenite, belite-larnite, alite-hatrurite (calcium silicates, calcium aluminosilicates and calcium
26 aluminates, in the 2.97–2.61 Å interval) rules out the presence of hydraulic binders and is therefore
27 indicative of aerial lime binders.
28
29
30
31
32
33
34
35
36
37
38
39
40
41
42
43
44
45
46
47
48
49
50
51
52
53
54
55
56
57
58
59
60
61
62
63
64
65

1
2
3
4
5
6
7
8
9
10
11
12
13
14
15
16
17
18
19
20
21
22
23
24
25
26
27
28
29
30
31
32
33
34
35
36
37
38
39
40
41
42
43
44
45
46
47
48
49
50
51
52
53
54
55
56
57
58
59
60
61
62
63
64
65

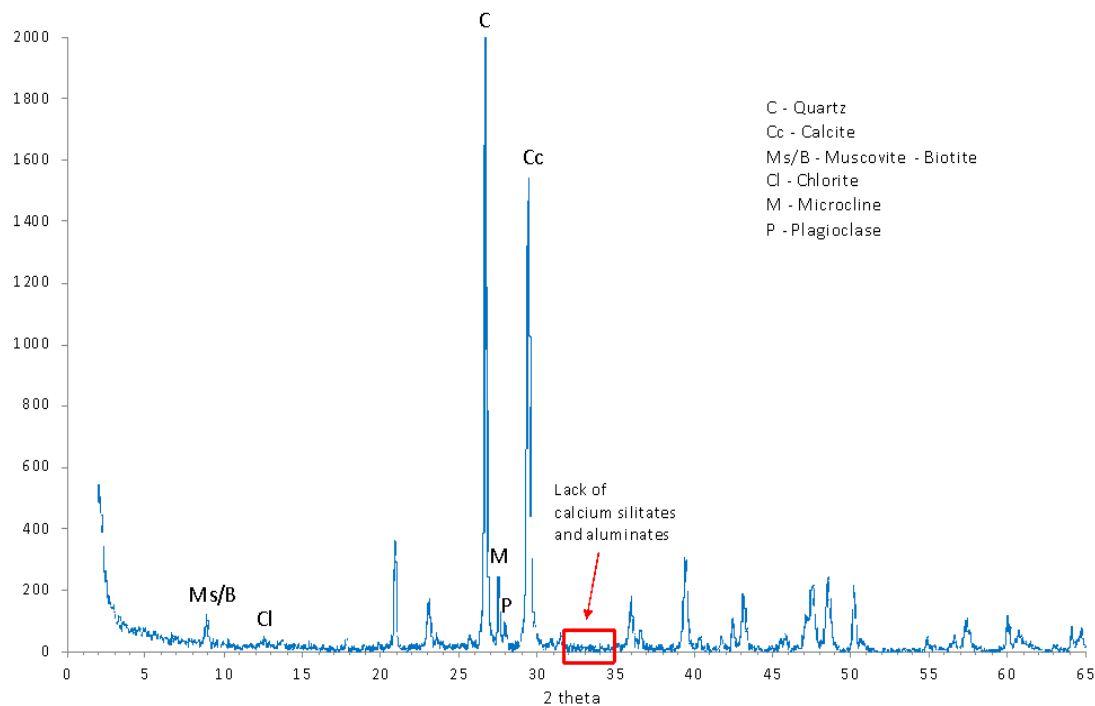


Figure 7. XRD pattern of a historic aerial lime mortar (17th century), total powder sample, without previous separation. The minerals identified are quartz and micas (muscovite, chlorite and biotite) and feldspars (microcline and plagioclase), which account for the aggregate mineralogy, as isolated minerals or in a rock fragment. The calcite identified corresponds to the binder, and not to the presence of carbonate aggregate (after confirmation by POM).

3.5. Chemical characterization

3.5.1. Thermal analyses

Thermal analysis (TA) is a group of techniques that study the changing crystallographic properties of materials as temperature changes. Thermogravimetric analysis (TGA) measures the mass change that a mineral undergoes with temperature, commonly while raising it up to 1200 °C in a controlled environment. Another thermal analysis is differential thermal analysis (DTA), in which the material under study and an inert reference are subjected to identical thermal cycles. Any temperature difference between the sample and the reference is recorded. In this technique, the heat flow to the sample and the reference remain the same rather than the temperature. It is a destructive technique in which 10 mg of ground sample is heated. TGA and DTA are used together (quantitative/semi-quantitative techniques) to perform chemical characterization and analyse the crystallographic thermal stability of mortar components (binder and aggregate) (Schueremans et al. 2011). Figure 8 shows an example of an aerial mortar analysed using TGA-DTA.

In aerial lime mortar, weight loss due to release of hygroscopic water occurs below 120 °C, release of interstitial water occurs up to 150 °C, water release in hydrated salts occurs between ~120 and ~200 °C and water chemically bound to the hydraulic phases is released at between ~200 and ~600 °C (Lawrence 2006; Genestar et al. 2006; Schueremans et al. 2011; Ergenç 2017). If the amount of the latter accounts for less than 3%, the mortar can be considered an aerial lime mortar (non-hydraulic) (Moropoulou et al. 2000). Weight loss above 600–650 °C is attributed to the release of carbon dioxide gas – CO₂ (decarboxylation process) – during CaCO₃ decomposition (Figure 8), although Bakolas et al. (1995) indicate that this decomposition can occur at lower temperatures (500–600 °C) when there are salts in the mortar. In addition, portlandite can also be detected (at between ~350 and ~450–550 °C) in historic mortars located in the inner parts of the masonry.

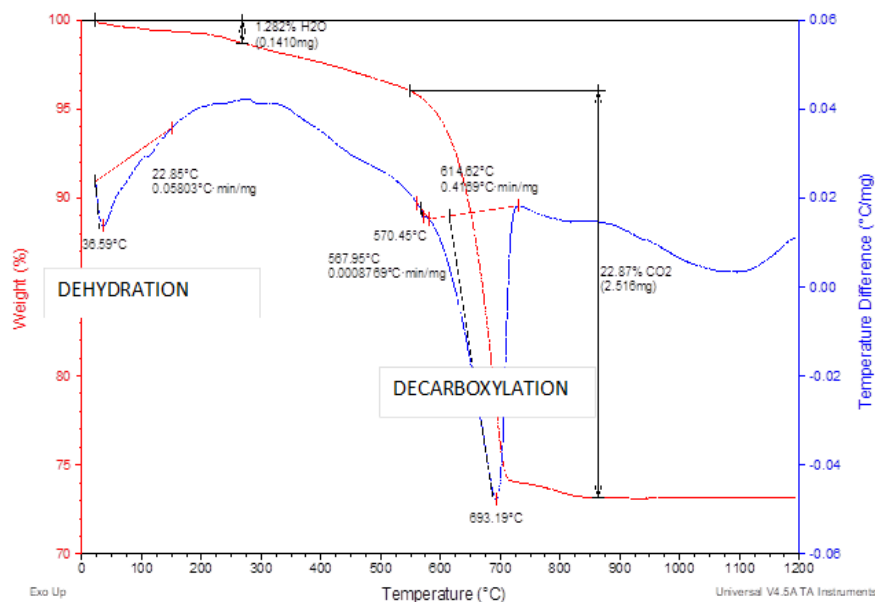


Figure 8. TGA/DTA thermal analysis of a historic aerial lime mortar from the 17th century. The red line refers to TGA and the blue line to DTA.

3.5.2. Chemical analyses using vibrational spectroscopy: Fourier-transform infrared spectroscopy

Fourier-transform infrared (FTIR) spectroscopy mainly makes it possible to identify the organic compounds intentionally added to these mortars (additives and admixtures), such as tallow, wax, nopal, animal glue, hair, blood, olive oil, linseed oil, egg, sticky rice, etc. (Yang et al 2009; Ingham 2011; Ventolá et al 2011; Zhang et al 2018; Artioli et al 2019). Detecting organics in historic mortars is not always possible since they decompose over time. FTIR also identifies inorganic functional groups, based on the vibration bands of the molecular bonds (Diekamp et al. 2012; Jordan et al. 2019).

1 Attenuated total reflectance (ATR) is a spectroscopic method frequently used with FTIR
2 spectrophotometers due to the advantages of its high accuracy, need for very little sample. For this
3 destructive technique, either pellets prepared using the KBr method (200 mg) or 1.5 mg of powdered
4 sample are needed. There are also handheld versions used to perform non-destructive testing in the
5 field. Although their accuracy is lower than that of laboratory equipment, they can be very useful in
6 situ as a means of discriminating/grouping samples and selecting the most adequate and
7 representative ones for analysis in the laboratory. The FTIR technique complements XRD analysis in
8 the characterization of historic mortars (Jordan et al. 2019).
9

10
11
12
13
14
15 When analysing these mortars, the resulting spectra allow the identification of the following minerals
16 (Figure 9) and organic compounds (Derrick, et al 1999; Farcas and Touzé, 2001; Park et al. 2002; Galván-
17 Ruiz and Velázquez-Castillo, 2011; database: The RRUFF™ Project, <https://rruff.info>):
18
19

- 20
21 - Calcite (carbonated binder, or carbonate aggregate) presents Ca-O stretching and bending
22 vibration bands mainly at 1450, 1800, 876 and 716 cm^{-1} .
23
- 24 - Quartz (aggregate) presents Si-O vibration bands at 1090–1050, 1160, 799–788, 699 and 530 cm^{-1} .
25
- 26 - Feldspars and micas (aluminium silicates, aggregates) show Si-Al, Al-O or Si-Al-Si vibration bands
27 at 1007, 800–700, 586 and 540 cm^{-1} (Figure 8).
28
- 29 - Portlandite, when present in more recent mortars or incomplete carbonated mortars, appears at
30 3640, 1470–1450 and 855 cm^{-1} , showing O-H (3640 cm^{-1}) and Ca-O (1470-1450 and 855 cm^{-1})
31 calcium hydroxide vibration bands.
32
- 33 - Structural and free water appears at 3440-3430 cm^{-1} (O-H) and at 1640-1620 cm^{-1} (H-O-H)
34
- 35 - Gypsum, either as a decay product or as an original raw material appears, with double bands, at
36 3525-3401 (O-H), 1682-1627 (H-O-H), 1145-1120 (S-O) and 670-600 (S-O) cm^{-1}
37
38
39
- 40
41 - Organic additions can be detected by the presence of the carbonyl (C=O) group absorption bands
42 between 1630 and 1750 cm^{-1} : 1740 cm^{-1} for ester, 1710 cm^{-1} for ketone, 1650 cm^{-1} for amide I,
43 1550 cm^{-1} for amide II and 1450 cm^{-1} for amide III. There is also a C-H stretching vibration double
44 band in the region of 3000–2800 cm^{-1} , which accounts for methyl (CH₃, 2962 and 2872 cm^{-1}) and
45 methylene (CH₂, 2926 and 2850 cm^{-1}) groups. Therefore, in the case of wax addition, there will be
46 stretching vibration double bands at 2926–2850, 1466–1462 and 730–720 cm^{-1} . When oil is
47 incorporated into the mortar mix, we expect to find bands at 1750–1740, 1464–1464, 1238–1244
48 and 1165–1154 cm^{-1} . When animal proteins are used, they can be detected at 1630–1680, 1520–
49 1560, 1450 and 1240 cm^{-1} (Derrick et al 1999).
50
51
52
53
54
55
56
57
58
59
60
61
62
63
64
65

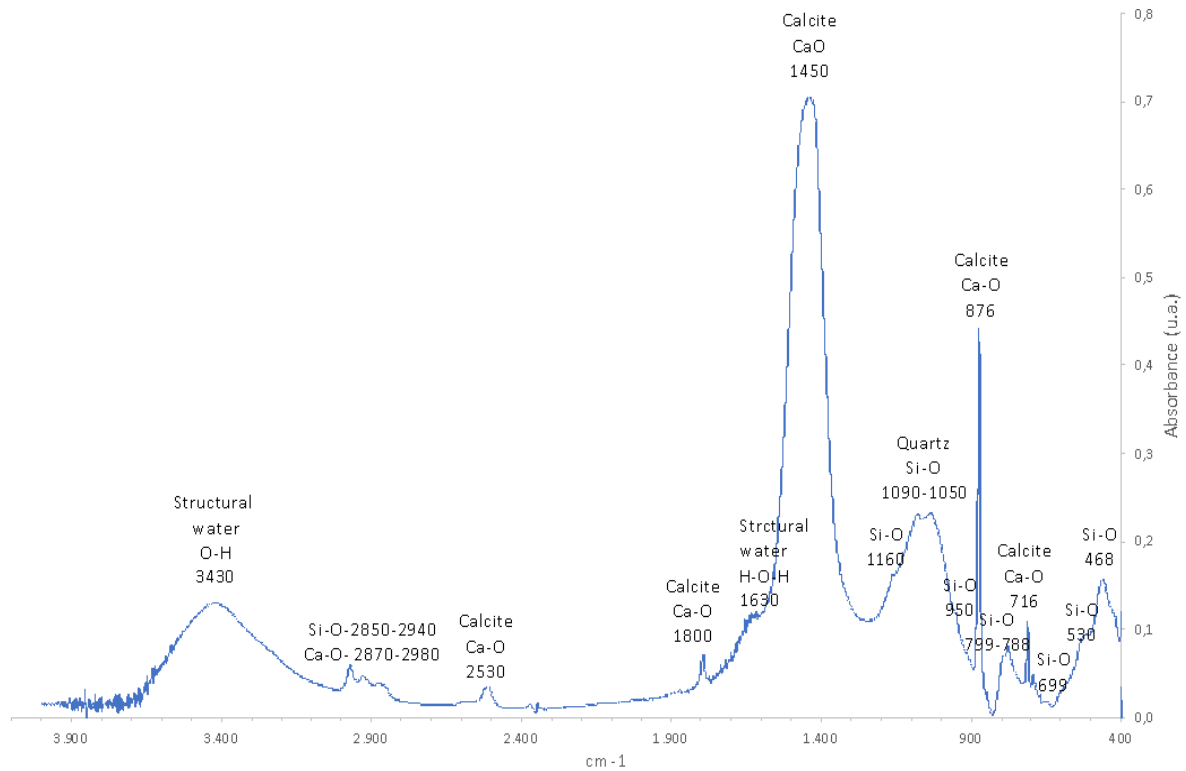


Figure 9. Interpreted FTIR spectrum of a historic aerial lime mortar from the 17th century.

3.5.3. Other techniques used in chemical analysis

X-ray fluorescence (XRF) investigates the chemical composition of and impurities in binders. The main purpose of this analysis is to identify quantitatively the elements of materials. An XRF spectrometer allows determination of the chemical composition of the major elements (SiO_2 , TiO_2 , Al_2O_3 , Fe_2O_3 , MnO , MgO , CaO , Na_2O , K_2O , P_2O_5) and trace elements (Ni, Cr, V, La, Ce, Co, Nb, Y, Sr, Zr, Cu, Zn, Rb) present in the mortar samples. In addition, loss on ignition (LOI) of the powdered samples provides insights into the degree of carbonation. The XRF samples of the powdered binder are analysed using a wavelength-dispersive XRF spectrometer (Miriello et al 2015). The use of portable XRF equipment allows direct measurements to be taken on mortars without the need for sampling. This technique has been introduced in recent years (Frahm and Donan 2013) due to its versatility and the results obtained, although they are semi-quantitative for materials such as mortar. Although the resolution of this portable technique is low, the results can be utilized for relative comparison of mortars (Donais et al 2020).

EDS analysis coupled to SEM (SEM-EDS) is a semi-quantitative analytical technique that can be performed on thin sections or bulk samples coated with conductive graphite, or without any metal sputtering when an EDS coupled to an environmental SEM (ESEM) is used, which makes it possible to use the mortar samples in further analyses. By means of EDS, analysis can be performed on a point, a line or an area, obtaining the results either as percentages of the corresponding chemical elements, or

1 as the calculated oxides of the elements. Note that EDS cannot detect elements less than 0.01 wt% or
2 low atomic number elements (until C). SEM-EDS has been successfully utilized to identify the
3 composition and texture of aggregates, lime lumps and binder (La Russa et al. 2015, Ricca et al. 2019),
4 and it is especially useful to confirm that the binder is an aerial one and to detect carbonatic aggregates
5 (Cultrone et al. 2005).
6
7
8
9

10 ○3.6. Stable Isotope analysis ($\delta^{13}\text{C}$ and $\delta^{18}\text{O}$)

11 In archaeometry, analysis of ^{13}C and ^{15}N isotopic content allows establishment of paleo-diets (Carvalho
12 and Petchey, 2013) or definition of population migrations by means of the strontium isotopic ratios
13 ($^{87}\text{Sr}/^{86}\text{Sr}$) that exist in the remains of analysed bones, teeth, hair, etc. (Frei et al. 2015). In lime mortars,
14 stable isotopes ^{13}C and ^{18}O are used to determine their history, including the manufacturing techniques
15 employed, together with the components used and their physico-chemical reactions during the
16 carbonation process, and the formation of secondary phases by the action of alteration or
17 recarbonation/crystallization (Dotsika et al. 2009, 2018).
18
19
20
21
22
23
24

25 For this analysis, small fragments of lime binder not subject to alteration processes are extracted from
26 the mortar sample with a scalpel. They are then ground and diluted in orthophosphoric acid and
27 analysed using a mass spectrometer. Isotope contents are defined as $\delta^{13}\text{C}$ and $\delta^{18}\text{O}$ using the isotopic
28 standard reference for VPDB carbonate (Cretaceous belemnites at Pee Dee, South Carolina, USA),
29
30
31
32

$$33 \delta = [(R_{\text{sample}} - R_{\text{standard}}) / R_{\text{standard}}] \times 1000$$

34 where R is the ratio of heavy isotope to light isotope, in this case $^{18}\text{O}/^{16}\text{O}$ or $^{13}\text{C}/^{12}\text{C}$.
35
36
37
38
39

40 Changes in the $\delta^{13}\text{C}$ and $\delta^{18}\text{O}$ isotopes are determined by the history of mortar: the manufacturing
41 techniques, together with the components used and their physico-chemical reactions during the
42 carbonation process, and the formation of secondary phases by the action of alteration or
43 recarbonation/crystallization (Dotsika et al. 2009, 2018). The content of the $\delta^{13}\text{C}$ isotope may indicate
44 the existence of geological carbonate – or incomplete calcination of the carbonate to make the lime –
45 and may overestimate the age of the mortar. It is thus possible to determine whether the lime was
46 made from marine or continental fossil remains as the $\delta^{13}\text{C}$ values will be between -1 and +4 ‰ and
47 between -8 and -12 ‰, respectively.
48
49
50
51
52
53
54

55 In addition, a lower $\delta^{13}\text{C}$ content may be due to recarbonation processes and, therefore, give more
56 recent ages. All this requires correction of the values (Van Strydonck et al. 1986; Ambers 1987;
57 Nawrocka et al. 2005).
58
59
60
61
62
63
64
65

1 The trend in the isotopic content during carbonation is towards enrichment of both isotopes to reach
2 the values of the limestone with which the mortars have been made, following the trend identified by
3 Kosednar-Legenstein et al. (2008).
4

5 However, isotope fractionation depends on many other factors, such as environmental conditions and
6 the type of mortar.
7

8 In alkaline environments, as is the case with fresh lime mortar, which is rich in portlandite, the values
9 are -25% for $\delta^{13}\text{C}$ and -20% for $\delta^{18}\text{O}$ (Kosednar-Legenstein et al. 2008). These values change as the pH
10 becomes more neutral during carbonation and portlandite transforms into calcite.
11
12

13 In areas of higher humidity, it is likely that more positive values of $\delta^{18}\text{O}$ and more negative values of
14 $\delta^{13}\text{C}$ will occur, favoured by increased biological activity (Åberg et al. 1995; Michalska and Pawlyta
15 2019).
16
17

18 Those changes in the isotopic evolution also makes it possible to establish whether the mixing water
19 used in production of the mortar was the same in the different construction phases, as well as to
20 identify differences in the raw materials used to produce the mortar (Ergenç et al. 2019). The existence
21 of consolidation and/or water-repellent treatments makes isotopic characterization of the mortars on
22 which they were applied unfeasible (Ergenç et al. 2019).
23
24
25
26
27

28 The presence of saline phases can lead to enrichment of $\delta^{18}\text{O}$ (Dotsika et al. 2018), although it depends
29 on the type of salt and its concentration, with the processes of dissolution and subsequent
30 recrystallization or cementation of calcitic phases having more influence (Fort et al. 2021).
31
32
33
34
35

36 ○ **3.7. Dating techniques**

37 One of the archaeological challenges is to establish the date of construction of the architectural
38 elements. Absolute dating of the mortars is crucial when it comes to specifying the phases of
39 construction. Mortar dating remains one of the most difficult problems to solve as regards obtaining
40 reliable results. Current research is trying to develop two techniques in particular: isotopic radiocarbon
41 (^{14}C) techniques and optically stimulated luminescence (OSL). Each of these techniques focuses on
42 different components of the mortar. Radiocarbon analyses the content of the ^{14}C isotope in the binder
43 matrix of the mortar, while OSL focuses on the aggregates.
44
45
46
47
48
49
50
51

52 ▪ **3.7.1. Radiocarbon dating**

53 This technique is based on the phenomenon that a certain amount of CO_2 is lost during the calcination
54 of carbonate rocks, generating CaO (see Gliozzo et al. 2021 in this TC for a basic description of the
55 method).
56
57
58
59
60
61
62
63
64
65

1 A large number of variables affect the dating of the binder or of the calcite formed, mainly concerning
2 the manufacturing technology: firing temperature, type of kiln, characteristics of the lime slaking water
3 and even the water for mixing the aggregates and the lime.
4

5 The most reliable datings are obtained in pure limes (calcitic) (Hajdas et al. 2017; Hayen et al. 2017).

6 Various sources of contamination of the carbonate phases, unrelated to the initial process of
7 carbonation of the lime matrix, can modify the dating of the mortar:
8

9
10 - Incomplete calcination of the raw material used to produce quicklime, leaving limestone fragments
11 insufficiently burnt as the kilns did not reach sufficient temperature (900 °C). This results in older
12 dating results. $\delta^{13}\text{C}$ fractionation has been used to estimate the amount of calcareous contamination
13 present in mortars (Van Strydonck et al. 1986; Ambers 1987). Fragments of rocks or fossils in
14 aggregates of a carbonate nature result in older dates.
15

16
17 - Dissolution and recrystallization of carbonate phases from the mortar itself or from other external
18 materials, which will give more recent dates.
19

20
21 - The presence of plant residues and coal from the combustion of wood in the kilns (Olsen et al. 2013),
22 or from additives incorporated to improve one or more properties of the mortar (Sickels 1981).
23

24
25 - Biological activity generates CO_2 that can modify isotopic fractionation and can also generate soluble
26 salts (Gómez Heras et al. 2004; Pérez-Alonso 2004), rejuvenating the age of the mortar (Lubrittoa et
27 al. 2018).
28

29
30 - Lime mortars damaged by fire undergo partial decarbonation, reactivating the process due to the CO_2
31 produced and providing more modern ages (Heinemeier et al. 2010; Lindroos et al. 2018).
32

33
34 It should be borne in mind that the mortar hardening process is relatively rapid compared to the
35 average life of ^{14}C (5730 ± 40 years), and that it is common for the setting of the surface of mortars to
36 be completed in months (Pachiaudi et al. 1986), while decades may pass before the entire volume of
37 the mortar is carbonated (Ambers 1987; Van Strydonck and Dupas 1991), causing variations in the
38 dating of the same element and offering younger ages for the non-carbonated parts. In the same way,
39 the application of coatings can delay the carbonation process of pointing mortars, resulting in more
40 recent dating (Pesce et al. 2009).
41
42
43
44
45
46
47

48
49 These conditions, which can be found at the archaeological site, necessitate proper selection of the
50 samples for analysis in order to obtain reliable results that allow correct interpretation. It is necessary
51 to have information provided by the archaeology of architecture (Gliozzo et al. 2021 in this TC) and to
52 use the sampling strategies established in Daugbjerg et al. 2020. Besides, for correct dating, it is
53 necessary to know the environmental conditions in which the mortars were found, e.g. buried,
54 submerged or subjected to water filtration. It is advisable to take samples from areas not too far from
55 the surface to ensure that they are carbonated (Lindroos et al. 2018; Daugbjerg et al. 2021), although
56
57
58
59
60
61
62
63
64
65

1
2
3
4
5
6
7
8
9
10
11
12
13
14
15
16
17
18
19
20
21
22
23
24
25
26
27
28
29
30
31
32
33
34
35
36
37
38
39
40
41
42
43
44
45
46
47
48
49
50
51
52
53
54
55
56
57
58
59
60
61
62
63
64
65

it should be borne in mind that most historic mortars are fully carbonated. It is very important to carry out prior petrological and mineralogical characterization of the mortars to be dated so as to ascertain the compounds and their influence on the results.

The methodology for carrying out radiocarbon dating analysis is presented in Hajdas et al. (2017) and Hayen et al. (2017). The methodology depends in many cases on the type of mortar, its components and possible existing contaminants. It is crucial to separate the anthropogenic carbonate from other lime carbonates, which can be done by acid hydrolysis, principally using orthophosphoric acid H_3PO_4 (Michalska 2019). The anthropogenic carbonate will react first, while the unburned carbonates will take longer to dissolve (Sonninen and Jungner 2001; Nawrocka et al. 2005; Lindroos et al. 2014). Another pre-treatment procedure is cryo-destruction (Nawrocka et al. 2005), which is based on light crushing, thermal breakage and sieving of the mortar before acid hydrolysis. Other methods are based on ultrasonic separation and subsequent sieving (Marzaioli et al. 2011; Lubritto et al. 2018; Nonni et al. 2018). In these methods, ^{14}C (with direct measurement of CO_2) is measured by mass spectrometry (MS). Currently, accelerator mass spectrometric (AMS) dating is performed after reduction to graphite, with the advantage of requiring much less sample quantity and much shorter analysis times (Heinemeier et al. 2010).

Dating the staged acid hydrolysis mortar makes it possible to determine the changes in CO_2 in five successive dissolution increments (Lindroos et al. 2007). Examples of these curves are shown in Figures 10a and 10b.

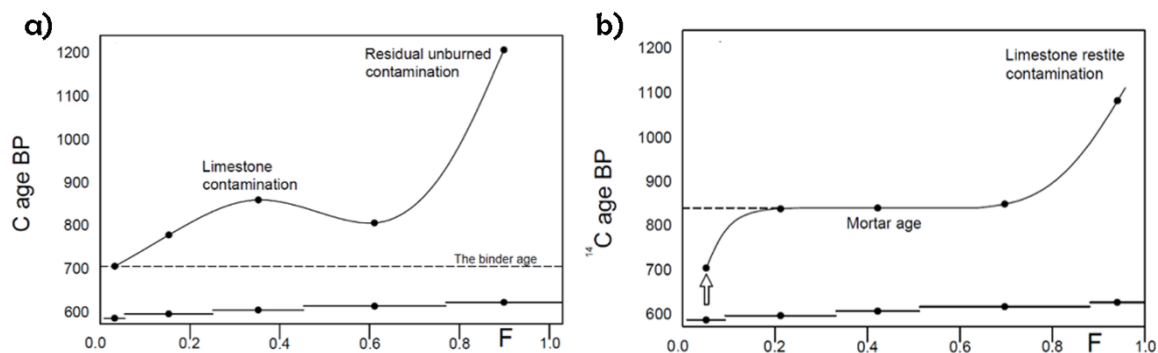


Figure 10. Carbonate dissolution profile (F) with mortar dating (dashed line). a) Effects of contamination of carbonate aggregate fragments and insufficiently burnt remains (adapted from Lindroos et al. 2014); b) Effects of fire on mortar or of re-carbonation/re-precipitation processes (the arrow marks the transformation of the mortar) (adapted from Heinemeier et al. 2010). C: Conventional radiocarbon age, BP: Before present

1
2
3
4
5
6
7
8
9
Appropriate selection of the mortar to be dated, new techniques for removing contaminants and the AMS dating technique create the prospect of increasingly accurate dating. The current scientific approach is to date lumps in the binder which, together with analysis of the binder, improve dating (Pesce et al. 2012, Lindroos et al. 2018).

▪ **3.7.2. Optically stimulated luminescence dating**

10
11
12
13
14
15
16
17
18
19
20
21
22
23
24
25
26
27
Dating of mortar using OSL is possible because over their geological history the quartz grains have received natural radiation from isotopes of thorium, uranium and potassium, as well as the ionizing action of cosmic rays, trapping electrons in crystalline defects in the minerals. Quartz and, to a lesser extent, feldspar are mainly used in OSL dating. When these minerals are extracted from quarries to be incorporated as aggregates in mortars the solar radiation they receive removes these trapped electrons. This process is called optical bleaching. When the quartz is incorporated into the mortar mix and, once it has been put in place, it once again receives the flow of radioactive particles (alpha α , beta β and gamma γ) from radioactive elements from other components in the environment in which it is found (other minerals in the mortar, such as zircons, biotites from granite ashlar or bricks), thereby steadily re-accumulating electrons in its structure in what is known as the annual dose.

28
29
30
31
32
33
34
35
36
37
38
39
40
41
The relationship between the dose accumulated since the last exposure to light, measured by the luminescence emitted, and the annual dose emitted in the immediate environment of the sample of mortar being analysed in the building or on the archaeological site gives us the age of the construction phase. The study of luminescence in minerals after optical stimulation for absolute dating was proposed by Huntley et al. (1985). Mortar was first dated using this technique by Bøtter-Jensen et al. (2000), and subsequently by several other authors (Zacharias et al. 2002; Goedicke 2003, 2011; Jain et al. 2004; Gueli et al. 2010; Panzeri 2013; Stella et al. 2013; Urbanova et al. 2015; Urbanová and Guibert 2017; Urbanová et al. 2018).

42
43
44
45
46
47
48
49
50
51
52
The first papers used the multi-grain technique (MG-OSL), which measures the radiation emitted by the set of grains in the sample. However, as not all grains have reached optical bleaching, they maintain a residual geological radiation that produces an older dating result (Jain et al. 2004, Sawakuchi et al. 2011). The single-grain technique (SG-OSL) has improved the results by measuring the luminescence signals emitted by each grain (Goedicke 2011). Reliable data on 85% are now being obtained (Guibert et al. 2020).

53
54
The problems in OSL dating lie in:

55
56
57
58
59
60
61
62
63
64
65
- The degree of bleaching and the presence of a residual dose due to insufficient exposure to solar radiation during extraction, transport, storage and mixing of the aggregate with the binder during the production of the mortar and its laying.

1
2 - The differing sensitivity of quartz grains to radiation, as this depends on defects and impurities in the
3 crystalline network of the quartz (Jacobs et al. 2013).

4 - The determination of the annual equivalent dose received by the sample from its environment due
5 to the presence of radioactive elements that emit luminescent signals.

6
7 In short, the sensitivity of quartz to OSL stimulus is associated with its geological origin and the intrinsic
8 conditions in which the mortar is found. Moreover, luminescence concentration may be influenced by
9 the environmental conditions to which the minerals were exposed, such as incessant cycles of solar
10 heating, radiation and whitening (Pietsch et al. 2008).

11
12 In the OSL data, it is also necessary to carry out prior studies of the mortars in order to determine the
13 characteristics of the aggregates (fundamentally on quartz and feldspar grains/crystals by POM), the
14 chemical composition of the components of the mortar (aggregates and binder by SEM-EDS), and
15 evaluate the luminescence properties of the binder (by CL), the distribution of the grain size of the
16 aggregates, and the distribution of the radiation emission β ~~beta-emissions~~ in the mortar matrix.

17
18 In general, approximately 100 g of the volume of the mortar not exposed to light makes it possible to
19 obtain between 200 and 500 mg, of which 5% may have sufficient bleached grains. Less than 8% of all
20 measured grains exhibit an OSL signal (Urbanová and Guibert 2017; Urbanova et al. 2020).

21
22 Although much progress has been made in OSL dating, there are still issues to resolve, such as the
23 preheating temperature during sample preparation and the most appropriate quartz grain size for
24 analysis.

25
26
27
28
29
30
31
32
33
34
35 Regarding practical issues (sample preparation, quantity/dimensions), the choice of the preheating
36 temperature is crucial to correct estimation of the equivalent dose. Some authors recommend
37 preheating between 180 and 200 °C (Jain et al. 2004; Goedicke 2011), while others propose 160–260 °C
38 (Kiyak and Canel 2006).

39
40
41
42 Bleaching seems to be better when analysing coarse quartz grains, between 200 and 250 μm (Goedicke
43 2003, Urbanova et al. 2015), although various authors report satisfactory results with finer grain sizes
44 (Bøtter-Jensen et al. 2000; Stella et al. 2013; Panzeria et al 2019).

45
46
47 In short, the reliability of dating archaeological structures based on mortar radiocarbon or OSL depends
48 on the type of mortar and its constituents. Aerial lime mortars without ceramic additives give none
49 sound results. Nevertheless, dating must always be supported by dating of other materials and other
50 dating techniques, together with archaeological stratigraphic data to ensure the reliability of the
51 results obtained. Mortar-dating technology is advancing and is obtaining good results when combined
52 with other dating techniques (Brainn et al. 2011; Urbanova and Guibert 2017; Stella et al. 2018;
53 Fernandez-Fernandez et al. 2019; Panzeri et al. 2019; Cantisani et al. 2021). It is worth adding that
54
55
56
57
58
59
60
61
62
63
64
65

1
2
3
4
5
6
7
8
9
10
11
12
13
14
15
16
17
18
19
20
21
22
23
24
25
26
27
28
29
30
31
32
33
34
35
36
37
38
39
40
41
42
43
44
45
46
47
48
49
50
51
52
53
54
55
56
57
58
59
60
61
62
63
64
65

although scholarly attention is increasing, those techniques cannot be applied in most archaeological research because of their high cost.

● 4. FINAL REMARKS

- Throughout the history of construction, aerial lime mortars and plasters have been employed due to the high local availability of the raw materials and the ease of access to them, to their easy and quick manufacture, to the good resulting quality and to their durability and compatibility.
- Their main properties are low mechanical strength, high deformation capacity (plasticity), good workability, low elasticity modulus, high permeability to water and high porosity.
- The archaeometric characterization techniques used make it possible to answer archaeological questions related to past technologies, raw material use and environmental conditions, since the alteration processes modify the properties of the mortars. This review presents the main methods for characterizing aerial mortars, including those used to determine physical, hydric, mechanical, petrographic, mineralogical and chemical properties, as well as isotopic analyses and dating analyses.
- Proper and representative sampling and an adequate method of separating the binder from the aggregates is necessary for accurate mortar characterization. However, in many cases, this separation of components may not be possible without damaging the binder to be characterized. If so, joint characterization should be performed using the most appropriate techniques.
- Physical testing of mortars predominantly encompasses the analysis of porosity because of its significant influence on some of mortars' chief properties. The most appropriate techniques for measuring porosity are described, as are those for colour recording and for determining ultrasound pulse velocity. Hydric properties can be determined by different water absorption tests: at atmospheric pressure, by capillarity, under vacuum, under low pressure, by water vapour permeability and by drying or water evaporation. Hydric properties are highly important because they provide information on the behaviour of mortars and, in particular, on that of their binders in response to internal circulation of water and its various dissolved ionic compounds.
- Mechanical characterization includes measuring the strength of the mortar (compression, tensile and shear strength), the elasticity modulus, drilling resistance, hardness and modulus of elasticity, this last one being calculated using ultrasound pulse velocity and density.
- Petrographic techniques are indispensable in identifying the constituents, the relationship between them and the changes they undergo, as well as in determining raw material provenance and lime and mortar manufacturing techniques. They make it possible to distinguish the different

1 construction phases, at both local and historical level, by identifying the changes undergone in the
2 different mortars. The main microscopic techniques used to study mortar petrography are
3 reviewed: stereomicroscopy, polarizing optical microscopy, scanning electron microscopy,
4 fluorescence microscopy and cathodoluminescence devices coupled to different microscopes.
5

- 6
- 7 ● Mineralogical characterization can be obtained by X-ray diffraction, with each mineral showing a
8 characteristic XRD pattern. This technique can be used with each of the components (aggregates
9 and binders), either separately or jointly. Generally, it is a complementary technique to
10 petrographic microscopy, and identifies well-crystallized mineralogical phases.
11
- 12 ● Chemical characterization of these mortars can be achieved by various techniques. Thermal
13 analyses play a discriminative role in detecting a binder's aerial nature, while calculating the
14 degree of carbonation of aerial mortars using thermal analysis provides archaeometric insights.
15 Fourier-transform infrared spectroscopy permits identification of both the organic and inorganic
16 compounds – mainly those related to the additives and binder – of these mortars. X-ray
17 fluorescence spectrometry, and EDS microanalysis coupled to SEM also contribute towards
18 determining the chemical elements constituting these materials. The nature and provenance of
19 the binder can be determined using EDS on the incompletely calcined main rock used in production
20 of mortar (lime lump).
21
- 22 ● Stable isotope ($\delta^{13}\text{C}$ and $\delta^{18}\text{O}$) analyses reveal if the processing technology changed between the
23 different construction phases. The processes of recrystallization and cementation, as well as the
24 presence of carbonate alteration products, can alter stable isotope content.
25
- 26 ● Regarding dating techniques, ^{14}C -based dating is more reliable in pure aerial mortars not
27 containing unburnt limestone fragments or additives. The current trend is to analyse lime lumps.
28 The OSL dating technique for quartz grains has evolved from multi-grain to single-grain analysis,
29 although it is still necessary to adjust some measurement conditions such as the size of the grains
30 to be selected. Dating reliability depends on the type of mortar and has to be previously supported
31 by sampling protocols and the use of analytical mortar characterization techniques to avoid
32 contamination of the samples. Whenever possible, use should be made of various dating
33 techniques.
34
- 35 ● All the techniques utilized complement one other. A recommended approach is to combine
36 laboratory analyses and measurements with on-site non-destructive and portable techniques; in
37 accordance with EN 17187 (2020) non-destructive methods are always preferable to destructive
38 methods if they can provide the required information.
39
40
41
42
43
44
45
46
47
48
49
50
51
52
53
54
55
56
57
58
59
60
61
62
63
64
65

Acknowledgements

This study was funded by the CLIMORTEC (BIA2014-53911-R) project, Ministry of Economy and Competitiveness of Spain, and the TOP Heritage (P2018/NMT-4372) project, Community of Madrid. The authors are indebted to the IGEO Petrophysical Laboratory and to the Applied Petrology in Heritage Conservation group (921349). The authors wish to acknowledge the professional support of the Open Heritage: Research and Society (PTI-PAIS) CSIC Interdisciplinary Thematic Platform. Manuscript is edited by Andrew Steel of Veritas Traducción y Comunicación, SL.

References

Åberg G, Löfvendahl R, Stijfhoorn D, Råheim A (1995) Provenance and weathering depth of carbonaceous Gotland sandstone by use of carbon and oxygen isotopes. *Atmos Environ* 29:781–789. DOI: 10.1016/1352-2310(94)00324-E

Aceto M (2021) The palette of organic colourants in wall paintings. *Archaeol Anthropol Sci* (this Topical Collection)

Affonso MTC (1996). Identification of lime plasters. *The Old Potter's Almanak* 4: 1–6.

Affonso MTC, Freiberg EP (2001) Neolithic lime plasters and pozzolanic reactions. Are they occasional occurrences? In R.M. Boehmer & J. Maran (Eds.), *Lux Orientis. Archaeologie zwischen Asien and Europa, Festschrift fur Havald Hauptmann zum 65 Geburtstag* (pp. 9–13). Rahden/Westfalia: Verlag Marie Leidorf GmbH

Alvarez JI, Navarro I, Garcõa Casadoss PJ (2000) Thermal, mineralogical and chemical studies of the mortars used in the cathedral of Pamplona (Spain). *Thermochim Acta* 365:177-187. DOI: 10.1016/S0040-6031(00)00624-9

Ambers J (1987) Stable carbon isotope ratios and their relevance to the determination of accurate radiocarbon dates for lime mortars. *J Archaeol Sci* 14:569-576. DOI: 10.1016/0305-4403(87)90076-8

Arandigoyen M, Alvarez JI (2007) Pore structure and mechanical properties of cement-lime mortars. *Cem Concr Res* 37:767-775. DOI: 10.1016/j.cemconres.2007.02.023

Arandigoyen M, Bernal JLP, López MAB, Alvarez JI (2005) Lime-pastes with different kneading water: pore structure and capillary porosity. *Appl Surf Sci* 25:1449–1459. DOI: 10.1016/j.apsusc.2005.02.145

Arizzi A, Cultrone G (2012) The difference in behaviour between calcitic and dolomitic lime mortars set under dry conditions: the relationship between textural and physical– mechanical properties. *Cem Concr Res* 42:818–826. DOI: 10.1016/j.cemconres.2012.03.008

1 Arizzi A, Cultrone G (2014) The water transfer properties and drying shrinkage of aerial lime based
2 mortars: an assessment of their quality as repair rendering materials. *Environ Earth Sci* 71:1699–1710.
3 DOI: 10.1007/s12665-013-2574-x
4

5 Arizzi A, Cultrone G (2021) Mortars and plasters - How to characterize hydraulic mortars. *Archaeol*
6 *Anthropol Sci* (this Topical Collection)
7

8
9 Artioli G, Secco M, Addis A (2019) The Vitruvian legacy: Mortars and binders before and after the
10 Roman world. In: Artioli G, Oberti R, editors. *The contribution of mineralogy to cultural heritage*. *EMU*
11 *Notes in Mineralogy* 20 (4): 151–202. DOI: 10.1180/EMU-notes.20.4
12
13

14
15 ASTM D4404 (2018) Standard test method for determination of pore volume and pore volume
16 distribution of soil and rock by mercury intrusion porosimetry
17

18
19 Bakolas A, Biscontin G, Contardi V, Franceschi E, Moropoulou A, Palazz D, Zendri E (1995)
20 Thermoanalytical research on traditional mortars in Venice. *Thermochimica Acta* 269-270: 817-828
21
22 DOI: 10.1016/0040-6031(95)02574-X
23

24
25 Balksten K, Nitz B, Hughes JJ, Lindqvist JE (2019) Petrography of historic mortar materials: Polarising
26 Light Microscopy as a Method for Characterising Lime-Based Mortars. *Proceedings of the 5th Historic*
27 *Mortars Conference*. HMC 2019. Navarra (Spain). ISBN: 9781510892439
28
29

30
31 Barbero-Barrera MM, García-Santos A, Neila-González FJ (2014) Thermal conductivity of lime mortars
32 and calcined diatoms, Parameters influencing their performance and comparison with the traditional
33 lime and mortars containing crushed marble used as renders. *Energ Buildings* 76:422–428.
34
35 DOI: 10.1016/j.enbuild.2014.02.065
36

37
38 Barnett WK (1991) Optical petrography as a tool for examining gypsum and lime plaster
39 pyrotechnology. *J Field Archaeol* 18 253–255. DOI: 10.1179/009346991792208290
40

41
42 Becker H (2021) Pigment nomenclature in the ancient Near East, Greece, and Rome. *Archaeol*
43 *Anthropol Sci* (this Topical Collection)
44

45
46 Bensted J (1997) *Cements - past, present and future*. Inaugural Lecture Series, University of Greenwich,
47 16 pp. Greenwich University Press, Dartford, Kent, UK
48

49
50 Beruto DT, Vecchiattini R, Giordani M (2003) Solid products and rate-limiting step in the thermal half
51 decomposition of natural dolomite in a CO₂ (g) atmosphere. *Thermochim Acta* 405:183–194. DOI:
52 10.1016/S0040-6031(03)00190-4
53

54
55 Biscontin G, Birelli MP, Zendri E (2002) Characterization of binders employed in the manufacture of
56 Venetian historical mortars. *J Cull Herit* 3:31–37. DOI: 10.1016/S1296-2074(02)01156-1
57
58
59
60
61
62
63
64
65

1 Blaeuer C, Kueng A (2007) Examples of microscopic analysis of historic mortars by means of polarising
2 light microscopy of dispersions and thin sections. *Mater Charact* 58:1199-1207.
3 DOI: 10.1016/j.matchar.2007.04.023
4

5 Blain S, Guibert P, Prigent D, Lanos P, Oberlin C, Sapin C, Bouvier A, Dufresne P (2011) Combined dating
6 methods applied to building archaeology: the contribution of thermoluminescence to the case of the
7 bell tower of St Martin's church, Angers (France). *Geochronometria* 38:55-63 DOI: 10.2478/s13386-
8 011-0010-0
9

10
11
12
13 Blezard RG (1998) The history of calcareous cements, In *Lea's Chemistry of Cement and Concrete* 4th,
14 ed, P, C, Hewlett, London UK: Arnold Publishers 1-23. ISBN: 978-0-7506-6256-7
15

16
17 Boggs S, Krinsley D (2006) Application of cathodoluminescence imaging to the study of sedimentary
18 rocks. Cambridge: Cambridge University Press. ISBN: 0-521-85878X
19

20
21 Borges C, Santos Silva A, Veiga, R (2014) Durability of ancient lime mortars in humid environment
22 *Constr Build Mater* 66:606-620. DOI: 10.1016/j.conbuildmat.2014.05.019
23

24
25 Bøtter-Jensen LM, Solongo S, Murray AS, Banerjee D, Jungner H (2000) Using OSL single-aliquot
26 regenerative-dose protocol with quartz extracted from building materials in retrospective dosimetry.
27 *Radiat Meas* 32:841–845. DOI: 10.1016/S1350-4487(99)00278-4
28
29

30
31 Böke H, Cizer Ö, İpekoğlu B, Uğurlu E, Şerifaki K, Toprak G (2008) Characteristics of lime produced from
32 limestone containing diatoms. *Construct Build Mater* 22:866-874.
33 DOI: 10.1016/j.conbuildmat.2006.12.010
34
35

36
37 Bugani S, Camaiti M, Morselli L, Van de Castele E, Janssens K (2007) Investigation on porosity changes
38 of Lecce stone due to conservation treatments by means of x-ray nano and improved micro-computed
39 tomography: preliminary results. *X-Ray Spectrom* 36:316-320. DOI: 10.1002/xrs.976
40
41

42
43 Bultreys T, Boone MA, Boone MN, De Schryver T, Masschaele B, Van Hoorebeke L, Cnudde V (2016)
44 Fast laboratory-based micro-computed tomography for pore-scale research: Illustrative experiments
45 and perspectives on the future. *Adv Water Resour* 95:341-351. DOI:
46 <https://doi.org/10.1016/j.advwatres.2015.05.012>
47
48

49
50 Burgio L (2021) Pigments, dyes and inks – their analysis on manuscripts, scrolls and papyri. *Archaeol*
51 *Anthropol Sci* (this Topical Collection)
52

53
54 Bustillo-Revuelta M, Durán-López A, Fueyo-Casado L, 2014. *Manual de áridos*. Fueyo editores. ISBN-
55 13: 978-849393917. ISBN-10: 849393917X. 600p.
56
57
58
59
60
61
62
63
64
65

1
2
3
4
5
6
7
8
9
10
11
12
13
14
15
16
17
18
19
20
21
22
23
24
25
26
27
28
29
30
31
32
33
34
35
36
37
38
39
40
41
42
43
44
45
46
47
48
49
50
51
52
53
54
55
56
57
58
59
60
61
62
63
64
65

Cantisani E, Calandra S, Barone S, Caciagli S, Fedi M, Garzonio CA, Liccioli L, Salvadori B, Salvatici T, Vettori S (2021) The mortars of Giotto's Bell Tower (Florence, Italy): raw materials and technologies. *Construct Build Mater* 267:120801. DOI: 10.1016/j.conbuildmat.2020.120801

Carò F, Di Giulio A, Marmo R (2006) Textural analysis of ancient plasters and mortars: reliability of image analysis approaches. In: Maggetti, M. & Messiga, B. (eds). *Geomaterials in Cultural Heritage*. Geological Society, London, Special Publications 257:337–345. DOI:10.1144/GSL.SP.2006.257.01.26

Carran D, Hughes J, Leslie A, Kennedy C (2012) A Short History of the Use of Lime as a Building Material Beyond Europe and North America. *International J Architect Herit* 6:117-146. DOI: 10.1080/15583058.2010.511694

Caroselli M, Ruffolo SA, Piqué F (2021) Mortars and plasters – How to manage mortars and plasters conservation. *Archaeol Anthropol Sci* (this Topical Collection)

Carvalho AF, Petchey F (2013) Stable Isotope Evidence of Neolithic Palaeodiets in the Coastal Regions of Southern Portugal. *J Island & Coastal Archaeol* 8(3):361-383. DOI: 10.1080/15564894.2013.811447

Casadio F, Chiari G, Simon S (2005) Evaluation of binder/ aggregate ratios in archaeological lime mortars with carbonate aggregate: a comparative assessment of chemical, mechanical and microscopic approaches. *Archaeometry* 47: 671-89. DOI: 10.1111/j.1475-4754.2005.00226.x

Cavallo G, Riccardi MP (forthcoming) Glass-based pigments in painting. *Archaeol Anthropol Sci* (this Topical Collection)

Cazalla O (2002) *Morteros de cal, Aplicación en el Patrimonio Histórico*, Tesis Doctoral, Universidad de Granada. Spain. 232 p

Cazalla O, Sebastian E, Cultrone G, Nechar M, Bagur MG (1999) Three-way ANOVA interaction analysis and ultrasonic testing to evaluate air lime mortars used in cultural heritage conservation projects. *Cem Concr Res* 29:1749-1752. DOI: 10.1016/S0008-8846(99)00158-1

Cazalla O, Rodriguez-Navarro C, Sebastian E, Cultrone G, de la Torre MJ (2004) Aging of Lime Putty: Effects on Traditional Lime Mortar Carbonation. *J Am Ceram Soc* 83:1070–1076. DOI: 10.1111/j.1151-2916.2000.tb01332.x

Chapoulie W, Cazenave S, Cerepi A (2005) Contribution of high-resolution cathodoluminescence to the meteoric diagenesis in sedimentary carbonates. *Comptes Rendus Geoscience* 3: 337-346. DOI: 10.1016/j.crte.2004.10.008

1
2
3
4
5
6
7
8
9
10
11
12
13
14
15
16
17
18
19
20
21
22
23
24
25
26
27
28
29
30
31
32
33
34
35
36
37
38
39
40
41
42
43
44
45
46
47
48
49
50
51
52
53
54
55
56
57
58
59
60
61
62
63
64
65

Costa D, Magalhães A, do Rosário Veiga M (2012) Characterisation of Mortars Using Drilling Resistance Measurement System (DRMS): Tests on Field Panels Samples. In *Historic Mortars* 413-423, Springer Dordrecht. DOI: 10.1007/978-94-007-4635-0_32

Cultrone G, Sebastián E, Huertas MO (2005) Forced and natural carbonation of lime-based mortars with and without additives: Mineralogical and textural changes. *Cem Concr Res* 35:2278-2289. DOI: 10.1016/j.cemconres.2004.12.012

Damas AN, Veiga MR, Faria P, Silva AS (2018) Characterisation of old azulejos setting mortars: A contribution to the conservation of this type of coatings. *Construct Build Mater* 171:128-139. DOI: <https://doi.org/10.1016/j.conbuildmat.2018.03.103>

Daugbjerg TS, Lindroos A, Heinemeier J, Ringbom A, Barrett G, Michalska D, Hajdas I, Raja R, Olsen J (2020) A field guide to mortar sampling for radiocarbon dating. *Archaeometry* (on line) DOI: 10.1111/arcm.12648

Degryse P, Elsen J, Waelkens M (2002) Study of ancient mortars from Sagalassos (Turkey) in view of their conservation. *Cem Concr Res* 32:1457–1463. DOI: 10.1016/S0008-8846(02)00807-4

De Laine J (2021) Production, transport and on-site organisation of Roman mortars and plasters. *Archaeol Anthropol Sci* (this Topical Collection)

Derrick MR, Stulik D, Landry JM (1999). *Infrared Spectroscopy in Conservation Science. Scientific Tools for Conservation*. Getty Publications. Getty Conservation Institute. UU.EE. 248p. ISBN 978-0-89236-469-5

Dickson JAD (1966) Carbonate identification and genesis revealed by staining. *J Sediment Petrol* 36:491-505.

Diekamp A, Stalder R, Konzett J, Mirwald PW (2012) Lime Mortar with Natural Hydraulic Components: Characterisation of Reaction Rims with FTIR Imaging in ATR-Mode. In: *Historic Mortars: Characterisation, Assessment and Repair*, J. Válek et al. (eds.), 105-113. DOI: 10.1007/978-94-007-4635-0

Divya Rani S, Rahul AV, Santhanam M (2021) A multi-analytical approach for pore structure assessment in historic lime mortars. *Constr Build Mater* 272:121905. DOI: <https://doi.org/10.1016/j.conbuildmat.2020.121905>

Domingo Sanz I, Chieli A (2021) Characterising the pigments and paints of prehistoric artists. *Archaeol Anthropol Sci* (this Topical Collection)

1
2
3
4
5
6
7
8
9
10
11
12
13
14
15
16
17
18
19
20
21
22
23
24
25
26
27
28
29
30
31
32
33
34
35
36
37
38
39
40
41
42
43
44
45
46
47
48
49
50
51
52
53
54
55
56
57
58
59
60
61
62
63
64
65

Donais MK, Alrais M, Konomi K, George D, Ramundt WH, Smith E (2020) Energy dispersive X-ray fluorescence spectrometry characterization of wall mortars with principal component analysis: Phasing and ex situ versus in situ sampling. *J Cult Herit* 43: 90-97. DOI: 10.1016/j.culher.2019.12.007

Dotsika E, Psomiadis D, Poutoukis D, Raco B, Gamaletsos P (2009) Isotopic analysis for degradation diagnosis of calcite matrix in mortar. *Anal Bioanal Chem* 395:2227–2234. DOI: 10.1007/s00216-009-3135-8

Dotsika E, Kyropoulou D, Christaras V, Diamantopoulos G (2018) ¹³C and ¹⁸O stable isotope analysis applied to detect technological variations and weathering processes of ancient lime and hydraulic mortars. *Geosciences* 8: 339. DOI: 10.3390/geosciences8090339

Drdácký M, Slížková Z (2007) Mechanical characteristics of historical mortars from tests on small-sample non-standard specimens, 3rd Baltic Conference on Silicate Materials – Book of Abstracts, 9-11, Riga Technical University.

Elsen J (2006) Microscopy of historic mortars—A review. *Cem Concr Res* 36:1416–24. DOI: 10.1016/j.cemconres.2005.12.006

Elsen J, Mertens G, Van Balen K (2011) Raw materials used in ancient mortars from the Cathedral of Notre-Dame in Tournai (Belgium). *Eur J Mineral* 23:871–882. DOI: 10.1127/0935-1221/2011/0023-2139

EN 1015 (2002) Methods of test for mortar for masonry. Part 18: Determination of water absorption coefficient due to capillary action of hardened mortar. European Committee for Standardization, Brussels, Belgium.

EN 1015 (2016) Methods of test for mortar for masonry. Part 12: Determination of adhesive strength of hardening and plastering mortars on substrates. European Committee for Standardization, Brussels, Belgium.

EN 1015 (2019) Methods of test for mortar for masonry. Part 11: Determination of flexural and compressive strength of hardened mortar. European Committee for Standardization, Brussels, Belgium.

EN 1936 (2006) Natural stone test methods - Determination of real density and apparent density, and of total and open porosity. European Committee for Standardization, Brussels, Belgium.

EN 12407 (2019) Natural stone test methods - Petrographic examination. European Committee for Standardization, Brussels, Belgium

1 EN 13755 (2008). Natural stone test methods - Determination of water absorption at atmospheric
2 pressure. European Committee for Standardization, Brussels, Belgium

3
4 EN 15801 (2009) Conservation of cultural property - Test methods - Determination of water absorption
5 by capillarity. European Committee for Standardization, Brussels, Belgium.
6

7
8 EN 15803 (2009) Conservation of cultural property - Test methods - Determination of water vapour
9 permeability. European Committee for Standardization, Brussels, Belgium
10

11
12 EN 16085 (2012) Conservation of Cultural property - Methodology for sampling from materials of
13 cultural property – General rules. European Committee for Standardization, Brussels, Belgium.
14

15
16 EN 16302 (2013) Conservation of cultural heritage - Test methods - Measurement of water absorption
17 by pipe method. European Committee for Standardization, Brussels, Belgium
18

19
20 EN 16322 (2013) Conservation of Cultural Heritage. Test methods. Determination of drying properties.
21 European Committee for Standardization, Brussels, Belgium
22

23
24 EN 16572 (2015) Conservation of cultural heritage. Glossary of technical terms concerning mortars for
25 masonry, renders and plasters used in cultural heritage. European Committee for Standardization,
26 Brussels, Belgium.
27

28
29
30 EN 17187 (2020) Conservation of cultural heritage. Characterization of mortars used in cultural
31 heritage. European Committee for Standardization, Brussels, Belgium.
32

33
34 Ergenç D (2017) Roman mortars used in the archaeological sites in Spain and Turkey: A Comparative
35 Study and the design of repair mortars, PhD Thesis, Universidad Politécnica de Madrid.
36 10.20868/UPM.thesis.48348
37

38
39
40 Ergenç D, Fort R (2018) Accelerating carbonation in lime-based mortar in high CO₂ environments,
41 Constr Build Mater 188:314-325. DOI: /10.1016/j.conbuildmat.2018.08.125
42

43
44 Ergenç D, La Russa MF, Ruffolo SA, Fort R, Sánchez Montes A (2018a) Characterization of the wall
45 paintings in La Casa de los Grifos of Roman city Complutum, Eur. Phys. J. Plus “New Challenges in the
46 Scientific Applications to Cultural Heritage” edited by M, Fedi L, Liccioli et al, 133: 355. DOI:
47 10.1140/epjp/i2018-12223-7
48

49
50
51 Ergenç D, Gomez Villalba LS, Fort R (2018b) Crystal development during carbonation of lime-based
52 mortars in different environmental conditions, Mater Charact 142:276-288. DOI:
53 10.1016/j.matchar.2018.05.043
54

55
56
57 Ergenç D, Fort R (2019) Multi-technical characterization of Roman mortars from Complutum Spain.
58 Measurement 147:106876. DOI: 10.1016/measurement.2019.106876
59
60
61
62
63
64
65

1 Farcas F, Touzé P (2001). La spectrométrie infrarouge à transformée de Fourier (IRTF). Une méthode
2 intéressante pour la caractérisation des ciments. Bulletin des Laboratoires des ponts et chaussées, 230:
3 77-88.
4

5 Fernandez-Fernandez A, Carvalho PC, Cristovao J, Sanjurjo-Sanchez J, Dias P (2019) Dating the early
6 Christian baptisteries from Idanha-a-Velha— the Suebi-Visigothic Egítania: stratigraphy, radiocarbon
7 and OSL. *Archaeol Anthropol Sci* 11:5691–5704. DOI: 10.1007/s12520-019-00901-9
8
9

10 Ferreira Pinto AP, Sena da Fonseca B, Vaz Silva D (2021) The role of aggregate and binder content in
11 the physical and mechanical properties of mortars from historical rubble stone masonry walls of the
12 National Palace of Sintra. *Constr Build Mater* 268:121080. DOI:
13 <https://doi.org/10.1016/j.conbuildmat.2020.121080>
14
15
16
17

18 Filomena CM, Hornung J, Stollhofen (2014) Assessing accuracy of gas-driven permeability
19 measurements: a comparative study of diverse Hassler-cell and probe permeameter devices. *Solid*
20 *Earth* 5:1-11. www.solid-earth.net/5/1/2014
21
22
23

24 Forster AM, Válek J, Hughes JJ & Pilcher N (2020) Lime binders for the repair of historic buildings:
25 Considerations for CO2 abatement. *J Clean Prod* 252:119802. DOI: 10.1016/j.jclepro.2019.119802
26
27

28 Fort R, Ergenç D, Aly N, Alvarez de Buergo M, Hemeda S (2021), Implications of new mineral phases in
29 the isotopic composition of Roman lime mortars at the Kom el-Dikka archaeological site in Egypt.
30 *Constr Build Mater* 268:121085. DOI: 10.1016/j.conbuildmat.2020.121085
31
32
33

34 Frahm E, Doonan RCP (2013) The technological versus methodological revolution of portable XRF in
35 archaeology. *J Archaeol Sci* 40: 1425-143. DOI: 10.1016/j.jas.2012.10.013
36
37

38 Frei K M, Mannering U, Douglas Price T, Birch Iversen R (2015) Strontium isotope investigations of the
39 Haraldskær Woman. *ArcheoSciences*, 39: 93-101. [10.4000/archeosciences.4407](https://doi.org/10.4000/archeosciences.4407)
40
41

42 Furlan V, Bissegger P (1975) Les mortiers anciens, Histoire et essais d'analyse scientifique. *Revue suisse*
43 *d'Art et d'Archéologie* 32: 1–14
44
45

46 Galván-Ruiz M, Velázquez-Castillo R. (2011). Lime, an ancient material as a renewed option for
47 construction. *Ingeniería, Investigación y Tecnología*, 7 (1): 93-103. ISBN I 405-7743 FI-UNAM
48
49

50 Genestar C, Pons C, Mas A (2006) Analytical characterisation of ancient mortars from the
51 archaeological Roman city of Pollentia (Balearic Islands, Spain). *Anal Chim Acta* 557: 373-379. DOI:
52 [10.1016/j.aca.2005.10.058](https://doi.org/10.1016/j.aca.2005.10.058)
53
54
55

56 Gliozzo E (2021) Pigments – Mercury-based red (cinnabar-vermilion) and white (calomel) and their
57 degradation products. *Archaeol Anthropol Sci* (this Topical Collection)
58
59
60
61
62
63
64
65

1 Gliozzo E, Burgio L (2021) Pigments – Arsenic-based yellows and reds. Archaeol Anthropol Sci (this
2 Topical Collection)

3
4 Gliozzo E, Ionescu C (2021) Pigments – Lead-based whites, reds, yellows and oranges and their
5 alteration phases. Archaeol Anthropol Sci (this Topical Collection)

6
7
8 Gliozzo E, Pizzo A, La Russa MF (2021) Mortars, plasters and pigments Research questions and
9 sampling criteria. Archaeol Anthropol Sci (this Topical Collection)

10
11
12 Goedicke C (2003) Dating historical calcite mortar by blue OSL: Results from known age samples. Radiat
13 Meas 37:409–415. DOI: 10.1016/S1350-4487(03)00010-6

14
15
16 Goedicke C (2011) Dating mortar by optically stimulated luminescence: A feasibility study.
17 Geochronometria 38 (1): 42–49. DOI: 10.2478/s13386-011-0002-0

18
19
20 Gómez Heras M, Benavente D, Álvarez de Buergo M, Fort R (2004) Soluble salt minerals from pigeon
21 droppings as potential contributors to the decay of stone based cultural heritage. Eur J Mineral 16:505-
22 509. DOI: 10.1127/0935-1221/2004/0016-0505

23
24
25
26 Goren Y, Goldberg P (1991) Petrographic thin sections and the development of Neolithic plaster
27 production in Northern Israel. J Field Archaeol 18:131–138. DOI: 10.1179/009346991791548735

28
29
30 Goren Y (2014) The operation of a portable petrographic thin-section laboratory for field studies. NYMS
31 Newsletter, 17 pp, New York Microscopical Society

32
33
34 Gourdin WH, Kingery WD (1975) The beginnings of pyrotechnology: Neolithic and Egyptian lime
35 plaster. J Field Archaeol 2:133–150. DOI: 10.1179/009346975791491277

36
37
38 Gueli AM, Stella G, Troja SO, Burrafato G, Fontana D, Ristuccia GM, Zuccarello AR (2010) Historical
39 buildings: Luminescence dating of fine grains from bricks and mortar, Il Nuovo. Cimento 125 B:719–
40 729. DOI: 10.1393/ncb/i2010-10892-4

41
42
43
44 Guibert P, Urbanová P, Javel JB, Guérin G (2020) Modeling light exposure of quartz grains during mortar
45 making: Consequences for optically stimulated luminescence dating. Radiocarbon 62:693-711. DOI:
46 10.1017/RDC.2020.34

47
48
49
50 Güney BA (2012) development of pozzolanic lime mortars for the repair of historic masonry. Doctoral
51 Thesis. Middle East Technical University,
52 <https://open.metu.edu.tr/bitstream/handle/11511/22662/index.pdf>

53
54
55
56 Guydader J, Denis A (1986) Propagation des ondes dans les roches anisotropes sous contrainte
57 evaluation de la qualité des schistes ardoisiers. Bull Eng Geol 33:49–55. DOI: 10.1007/BF02594705

1 Hajdas I, Lindroos A, Heinemeier J, Ringbom Å, Marzaioli F, Terrasi F, Passariello I, Capano M, Artioli G,
2 Addis A, Secco M, Michalska D, Czernik J, Goslar T, Hayen R, Van Strydonck M, Fontaine L, Boudin M,
3 Maspero F, Panzeri L, Galli A, Urbanová P, Guibert P (2017) Preparation and dating of mortar samples
4 - Mortar Dating Intercomparison Study (MODIS). Radiocarbon 59:1845-1858. DOI:
5 10.1017/RDC.2017.112
6

7
8
9 Hayen R, Van Strydonck M, Fontaine L, Boudin M, Lindroos A, Heinemeier J, Ringbom Å, Michalska D,
10 Hajdas I, Hueglin S, Marzaioli F, Terrasi F, Passariello I, Capano M, Maspero F, Panzeri L, Galli A, Artioli
11 G, Addis A, Secco M, Boaretto E, Moreau Ch, Guibert P, Urbanová P, Czernik J, Goslar T (2017) Mortar
12 dating methodology: Assessing recurrent issues and needs for other research. Radiocarbon 59:1859–
13 1871. DOI: 10.1017/RDC.2017.129.
14
15

16
17
18 Heinemeier J, Ringbom Å, Lindroos A, Sveinbjörnsdóttir ÁE (2010) Successful AMS 14C dating of non-
19 hydraulic lime mortars from the medieval churches of the Åland islands Finland. Radiocarbon 52:171–
20 204. DOI: 10.1017/S0033822200045124
21
22

23
24 Hiatt EE, Pufahl PK (2014) Cathodoluminescence petrography of carbonate rocks: application to
25 understanding diagenesis, reservoir quality and pore system evolution. In: Coulson I (ed.)
26 Cathodoluminescence and its application to geoscience: Mineralogical Association of Canada, Short
27 Course Series 45:75-96.
28
29

30
31
32 Hughes JJ, Cuthbert SJ (2000) The petrography and microstructure of medieval lime mortars from the
33 west of Scotland: Implications for the formulation of repair and replacement mortars. Mater Struct
34 33:594-600. DOI: 10.1007/BF02480541
35
36

37
38 Hughes JJ, Leslie AB and Callebaut K (2001) The petrography of lime inclusions in historic lime based
39 mortars, Annales Geologiques des pays Helleniques, Edition Speciale, Volume XXXIX, ISSN: 1105-004,
40 359-364.
41
42

43
44 Huntley DJ, Godfrey-Smith DI, Thewalt MLW (1985) Optical dating of sediments. Nature 313:105-107.
45 DOI: 10.1038/313105a0
46

47
48 Hurd JD, Thompson D, Schmidt K (2011) Göbekli Tepe: Turkey Preliminary Site Conservation Inspection
49 and First Mortar and Plaster Documentation Report, San Francisco: Global Heritage Fund, 23 p. URL:
50 http://ghn.globalheritagefund.com/uploads/documents/document_2018.pdf
51

52
53
54 Ingham J (2011) Geomaterials under the microscope. A colour guide. Manson Publishing. London.
55 192p. ISBN: 978-1-84076-132-0
56

57
58 Jacobs Z, Hayes EE, Roberts GR, Galbraith RF, Henshilwood CS (2013) An improved OSL chronology for
59 the Still Bay layers at Blombos Cave South Africa: further tests of single-grain dating procedures and a
60
61
62
63
64
65

re-evaluation of the timing of the Still Bay industry across southern Africa. *J Archaeol Sci* 40:579–594.

DOI: 10.1016/j.jas.2012.06.037

Jain M, Thomsen KJ, Bøtter-Jensen L, Murray AS (2004) Thermal transfer and apparent-dose distributions in poorly bleached mortar samples: results from single grains and small aliquots of quartz.

Radiat Meas 38:101–109. DOI: 10.1016/j.radmeas.2003.07.002

Jordan NM, Jordá J, Pardo F, Montero MA (2019) Mineralogical analysis of historical mortars by FTIR. *Materials* 12:55. DOI: 10.3390/ma12010055

Karkanas P (2007) Identification of lime plaster in prehistory using petrographic methods: A review and reconsideration of the data on the basis of experimental and case studies. *Geoarchaeology* 22:775–796. DOI: 10.1002/gea.20186

Kingery WD, Vandiver PB, Prickett M (1988). The beginnings of pyrotechnology, part II: Production and use of lime and gypsum plaster in the Pre-Pottery Neolithic Near East. *J Field Archaeol* 15:219–244. DOI: 10.2307/530304

Kingery WD (1991) Optical petrography—Reply to Barnett. *J Field Archaeol* 18:255–256. DOI: 10.1179/009346991792208317

Kiyak NG, Canel T (2006) Equivalent dose in quartz from young samples using the SAR protocol and the effect of preheat temperature. *Radiat Meas* 41: 917–922. DOI: 10.1016/j.radmeas.2006.04.006.

Knapp CW, Christidis GE, Venieri D, Gounaki I, Gibney-Vamvakari J, Stillings M, Photos-Jones E (2021) The ecology and bioactivity of some Greco-Roman medicinal minerals: the case of Melos earth pigments. *Archaeol Anthropol Sci* (this Topical Collection)

Kosednar-Legenstein M, Dietzel A, Leis K (2008) Stable carbon and oxygen isotope investigation in historical lime mortar and plaster – results from field and experimental study. *Appl Geochem* 23:2425–2437. DOI: 10.1016/j.apgeochem.2008.05.003

Lancaster LC (2021) Mortars and Plasters - How mortars were made. The literary sources. *Archaeol Anthropol Sci* [this Topical Collection]

La Russa MF, Ruffolo SA (2021) Mortars and plasters - How to characterise mortars and plasters degradation. *Archaeol Anthropol Sci* (this Topical Collection)

La Russa MF, Ruffolo SA, Ricca M, Rovella N, Comite V, Alvarez de Buergo M, Barca D, Crisci GM (2015) Archaeometric approach for the study of mortars from the underwater archaeological site of Baia (Naples) Italy: Preliminary results. *Period Mineral* 84:553–567. DOI: 10.2451/2015PM0031

1
2
3
4
5
6
7
8
9
10
11
12
13
14
15
16
17
18
19
20
21
22
23
24
25
26
27
28
29
30
31
32
33
34
35
36
37
38
39
40
41
42
43
44
45
46
47
48
49
50
51
52
53
54
55
56
57
58
59
60
61
62
63
64
65

Lawrence M (2006) A study of carbonation in non-hydraulic lime mortars, Doctoral Thesis, University of Bath 344 pp.

Leslie AB, Hughes JJ (2002) Binder microstructure in lime mortars: implications for the interpretation of analysis results. *Q J Eng Geol Hydrogeol* 35:257–263. DOI: 10.1144/2F1470-923601-27

Lindqvist JE, Sandström M (2000) Quantitative analysis of historical mortars using optical microscopy. *Mater Struct* 33:612-617. DOI: 10.1007/BF02480600

Lindroos A (2005) Carbonate phases in historical building mortars and pozzolana concrete. Implications for AMS 14C dating PhD thesis. Åbo Akademi University.

Lindroos A, Heinemeie J, Ringbom Å, Braskén M, Sveinbjörnsdóttir Á (2007) Mortar dating using AMS 14C and sequential dissolution: examples from medieval non-hydraulic lime mortars from the Å land islands SV Finland. *Radiocarbon* 49:47–67. DOI: 10.1017/S0033822200041898

Lindroos A, Orsel E, Heinemeier J, Lill JO, Gunnelius K (2014) Radiocarbon dating of Dutch mortars made from burned shells. *Radiocarbon* 56:959-968. DOI: 10.2458/56.16508

Lindroos A, Ringbom Å, Heinemeier J, Hodgins G, Sonck-Koota P, Sjöberg P, Lancaster L, Kaisti R, Brock F, Ranta H, Caroselli M, Lugli S (2018) Radiocarbon dating historical mortars: lime lumps and/or binder carbonate? *Radiocarbon* 60:875–899. DOI: 10.1017/RDC.2018.17

López AJ, Pozo-Antonio JS, Ramil A, Rivas T (2018) Influence of the commercial finishes of ornamental granites on roughness, colour and reflectance. *Constr Build Mater* 182:530-540. DOI: 10.1016/j.conbuildmat.2018.06.144

Lubelli B, Nijland TG, Van Hees RPJ (2011) Self-healing of lime based mortars: microscopy observations on case studies. *Heron* 56 (1/2), <http://resolver.tudelft.nl/uuid:ff226ad0-ffb2-4b4c-bdb6-9881961bc7f1>

Lubritto C, Ricci P, Germinario C, Izzo F, Mercurio M, Langella A, Salvatierra Cuenca V, Montilla Torres I, Fedi M, Grif C (2018) Radiocarbon dating of mortars: Contamination effects and sample characterisation. The case-study of Andalusian medieval castles (Jaén Spain). *Measurement* 118:362-371. DOI: 10.1016/j.measurement.2017.10.046

Machel HG (2000) Application of cathodoluminescence to carbonate diagenesis. In: Pagel, M., Barbin, V., Blanc, P., Ohnenstetter, D. (Eds.), *Cathodoluminescence in Geosciences*. Springer-Verlag, Berlin, pp. 271-301. DOI: 10.1007/978-3-662-04086-7_11

1
2
3
4
5
6
7
8
9
10
11
12
13
14
15
16
17
18
19
20
21
22
23
24
25
26
27
28
29
30
31
32
33
34
35
36
37
38
39
40
41
42
43
44
45
46
47
48
49
50
51
52
53
54
55
56
57
58
59
60
61
62
63
64
65

Magalhães, Ana & Veiga, Maria. (2009). Physical and mechanical characterisation of historic mortars. Application to the evaluation of the state of conservation. *Mater de Construcción*. 59. DOI: <https://doi.org/10.3989/mc.2009.41907>

Marzaioli F, Lubritto C, Nonni S, Passariello I, Capano M, Terrasi F (2011) Mortar Radiocarbon dating: preliminary accuracy evaluation of a novel methodology. *Anal Chem* 83:2038–2045. DOI: 10.1021/ac1027462

Mastrotheodoros GP, Beltsios KG, Bassiakos Y (forthcoming) Pigments – Iron-based red, yellow and brown ochres. *Archaeol Anthropol Sci* (this Topical Collection)

Michalska D, Czernik J (2015) Carbonates in leaching reactions in context of ¹⁴C dating. *Nucl Instrum Meth B* 361:431–439. DOI: 10.1016/j.nimb.2015.08.033

Michalska D (2019) Influence of different pretreatments on mortar dating results. *Nucl Instrum Meth B: Beam Interactions with Materials and Atoms* 456:236–246. DOI: 10.1016/j.nimb.2019.03.038

Michalska D, Pawlyta J (2019) Modeled and measured carbon isotopic composition and petrographically estimated binder-aggregate ratio-recipe for binding material dating? *Radiocarbon* 61:799-815. DOI: 10.1017/RDC.2019.29

Middendorf BJJ, Hughes K, Callebaut G, Baronio I, Papayianni I (2005) Investigative Methods for the Characterization of Historic Mortars, Part 1: Mineralogical Characterisation. *Mater Struct* 38:761–69. DOI: 10.1007/BF02479289

Miriello D, Antonelli F, Apollaro C, Bloise A, Bruno N, Catalano M, Columbu S, Crisci, GM, De Luca R, Lezzerini M, Mancuso S, La Marca, A (2015) A petro-chemical study of ancient mortars from the archaeological site of Kyme (Turkey). *Period Mineral* 84:497-517. DOI: 10.2451/2015PM0028

Mopoulou A, Bakolas A, Bisbikou K (2000) Investigation of the Technology of Historic Mortars. *J Cult Herit* 1:45–58. DOI: 10.1016/S1296-2074(99)00118-1

Mota-López MA, Fort R, Álvarez de Buergo M, Pizzo A, Maderuelo-Sanz R, Meneses-Rodríguez JM, Ergenç D (2016). Characterization of concrete from Roman buildings for public spectacles in Emerita Augusta (Mérida, Spain). *Archaeol Anthropol Sci* 10:1007-1022. DOI: 10.1007/s12520-016-0434-9

Murakami T, Hodgins G, Simon AW (2013) Characterization of lime carbonates in plasters from Teotihuacan, Mexico: preliminary results of cathodoluminescence and carbon isotope analyses. *J Archaeol Sci* 40:960-970. DOI: 10.1016/j.jas.2012.08.045

Murat Z (2021) Wall paintings through the ages. The medieval period (Italy, 12th-15th century). *Archaeol Anthropol Sci* (this Topical Collection)

1
2
3
4
5
6
7
8
9
10
11
12
13
14
15
16
17
18
19
20
21
22
23
24
25
26
27
28
29
30
31
32
33
34
35
36
37
38
39
40
41
42
43
44
45
46
47
48
49
50
51
52
53
54
55
56
57
58
59
60
61
62
63
64
65

Nawrocka D, Michniewicz J, Pawlyta J, Padzur A (2005) Application of Radiocarbon method for dating of lime mortars. *Geochronometria* 24:109–115. DOI: 10.151/eochr-2015-0050

Nawrocka DM, Czernik J, Goslar T (2009) ¹⁴C dating of carbonate mortars from Polish and Israeli sites. *Radiocarbon* 51:857–866. DOI: 10.1017/S0033822200056162

Nonni S, Marzaioli F, Mignardi S, Passariello I, Capano M, Terrasi F (2018) Radiocarbon dating of mortars with a Pozzolana aggregate using the Cryo2SoniC protocol to isolate the binder. *Radiocarbon* 60:617–63. DOI: 10.1017/RDC.2017.116

Olsen J, Heinemeier J, Hornstrup KM, Bennike P, Thrane H J (2013) Old wood' effect in Radiocarbon dating of prehistoric cremated bones? *Archaeol Sci* 40:30-34. DOI: 10.1016/j.jas.2012.05.034

Ordoñez S, Fort R, García del Cura MA (1997) Pore size distribution and the durability of a porous limestone. *Q J Engin Geol* 30:221-230. DOI: 10.1144/GSL.QJEG.1997.030.P3.04

Pachiaudi C, Marechal J, Vanstrydonck M, Dupas M, Dauchotdehon M (1986) Isotopic fractionation of carbon during CO₂ absorption by mortar. *Radiocarbon* 28:691-697. DOI: 10.1017/S0033822200007906

Panzeri L (2013) Mortar and surface dating with optically stimulated luminescence (OSL): Innovative techniques for the age determination of buildings. *Nuovo Cimento* 36:205–216. DOI: 10.1393/ncc/i2013-11555-9

Panzeri L, Caroselli M, Galli A, Lugli S, Martini M, Sibilìa E (2019) Mortar OSL and brick TL dating: The case study of the UNESCO world heritage site of Modena. *Quaternary Geochronology* 49: 236-241. DOI: 10.1016/j.quageo.2018.03.005

Park J, Min D, Song H (2002). Structural Investigation of CaO–Al₂O₃ and CaO–Al₂O₃–CaF₂ Slags Via Fourier Transform Infrared Spectra. *ISIJ International*, 42(1):441–445. DOI: <https://doi.org/10.2355/isijinternational.42.38>

Pavía S, Caro S (2006) Origin of Films on Monumental Stone. *Stud Conserv* 51:177-188. www.jstor.org/stable/20619446

Pavía S, Caro S (2007) Petrographic microscope investigation of mortar and ceramic technologies for the conservation of the built heritage. In *Optics for Art, Architecture and Archaeology*. C. Fotakis, C., Pezzati, L., Salimbeni, R. Ed. Proc. Of SPIE, vol 6618, 66181H, 12p. Munich. DOI: 10.1117/12.726186

Pavía S, Caro S (2008) An investigation of Roman mortar technology through the petrographic analysis of archaeological material. *Constr Build Mater* 22:1807-1811. DOI: 10.1016/j.conbuildmat.2007.05.003

1 Pecchioni E, Fratini F, Cantisani E (2013) Atlas of the Ancient Mortars in thin section under optical
2 microscope. Nardini editore. Kermesquaderni. 102p. ISBN: 978-88-404-4366-9

3
4 Pérez-Alonso M, Castro K, Álvarez M, Madariaga JM (2004) Scientific analysis versus restorer's
5 expertise for diagnosis prior to a restoration process: the case of Santa Maria Church (Hermo Asturias
6 North of Spain). *Anal Chim Acta* 524:379–389. DOI: 10.1016/j.aca.2004.06.034

7
8
9 Pérez-Arantegui J (2021) Not only wall paintings – Pigments for cosmetics. *Archaeol Anthropol Sci* (this
10 Topical Collection)

11
12
13 Pesce G, Quarta G, Calcagnile L, Elia MD, Cavaciocchi P, Lastrico C, Guastella R (2009) Radiocarbon
14 dating of lumps from aerial lime mortars and plasters: methodological issues and results from San
15 Nicolò of Capodimonte church (Camogli, Genoa, Italy). *Radiocarbon* 51:867–872. DOI:
16 10.1017/S0033822200056174

17
18
19
20
21 Pesce GLA, Ball RJ, Quarta G, Calcagnile L (2012) Identification extraction and preparation of reliable
22 lime samples for 14 c dating of plasters and mortars with the "pure lime lumps" technique.
23 *Radiocarbon* 54:933-942. DOI: 10.1017/S0033822200047573

24
25
26
27 Pietch TJ, Olley JM, Nanson G (2008) Fluvial transport as a natural luminescence sensitiser of quartz.
28 *Quaternary Geochronology* 3:365–376. DOI: 10.1016/j.quageo.2007.12.005

29
30
31 Pinto APF, Nogueira R, Gomes A (2012) In Situ Techniques for the Characterisation of Rendering
32 Mortars. In *Historic Mortars* pp, 425-434, Springer Dordrecht. DOI: 10.1007/978-94-007-4635-0_33

33
34
35 Ponce-Antón G, Ortega LA, Zuluaga MC, Alonso-Olazabal A, Solaun JL (2018) Hydrotalcite and
36 Hydrocalumite in Mortar Binders from the Medieval Castle of Portilla (Álava, North Spain): Accurate
37 Mineralogical Control to Achieve More Reliable Chronological Ages. *Minerals* 8:326. DOI:
38 10.3390/min8080326

39
40
41
42 Radonjic M, Hallam KR, Allen GC, Hayward RJ (2001). The mechanism of carbonation in lime-based
43 mortars. Mechanism of carbonation in lime-based materials, Proceedings of the 8th Euroseminar on
44 Microscopy Applied to Building Materials, Athens (Greece), 2001, pp. 465 – 475.

45
46
47
48 Rafanelli S, Moita P, Mirao J, Carvalho A, Braga P, Vicente R, Galacho C, Barrocas Dias C, Candeias A,
49 Beltrame M, Coradeschi G (2017) Render mortars from Domus dei Dolia (Vetulonia, Italy) in
50 Programme and abstracts of Technoheritage 2017, MA Rogerio-Candelera, MJ Mosquera, ML
51 Almoraima Gil (eds) Spain. p178. URL: <http://hdl.handle.net/10174/22345>. ISBN: 978-1138067448

52
53
54
55
56 Ricca M, Galli G, Ruffolo SA, Sacco A, Aquino M, La Russa MF (2019) An archaeometric approach of
57 historical mortars taken from Foligno City (Umbria, Italy): news insight of Roman Empire in Italy.
58 *Archaeol Anthropol Sci* 11:1-9. DOI: 10.1007/s12520-018-0706-7

59
60
61
62
63
64
65

1
2
3
4
5
6
7
8
9
10
11
12
13
14
15
16
17
18
19
20
21
22
23
24
25
26
27
28
29
30
31
32
33
34
35
36
37
38
39
40
41
42
43
44
45
46
47
48
49
50
51
52
53
54
55
56
57
58
59
60
61
62
63
64
65

Rodrigues JD, Pinto AF, Da Costa DR (2002) Tracing of decay profiles and evaluation of stone treatments by means of microdrilling techniques. *J Cult Herit* 3:117-125. DOI: 10.1016/S1296-2074(02)01172-X

Rodriguez CR, Deprez M, de Mendonca Filho FF, van Offenwert S, Cnudde V, Schlangen E, Šavija B (2020) X-Ray Micro Tomography of Water Absorption by Superabsorbent Polymers in Mortar. In: Boshoff W., Combrinck R., Mechtcherine V., Wyrzykowski M. (eds) 3rd International Conference on the Application of Superabsorbent Polymers (SAP) and Other New Admixtures Towards Smart Concrete. SAP 2019. RILEM Bookseries, vol 24. Springer, Cham. DOI: 10.1007/978-3-030-33342-3_4

Sallam A, Hamed S, Toprak MS, Muhammed M, Hassa M, Uheida A (2019) CT Scanning and MATLAB Calculations for Preservation of Coptic Mural Paintings in Historic Egyptian Monasteries. *Sci Rep* 9:3903. DOI: 10.1038/s41598-019-40297-z

Salvadori M, Sbroli C (2021) Wall paintings through the ages. The Roman period: Republic and early Empire. *Archaeol Anthropol Sci* (this Topical Collection)

Sawakuchi AO, Blair MW, DeWitt R, Faleiros FM, Hyppolito T, Guedes CCF (2011) Thermal history versus sedimentary history: OSL sensitivity of quartz grains extracted from rocks and sediments. *Quat Geochronol* 6:261–272. DOI: 10.1016/j.quageo.2010.11.002

Schafer J, Hilsdorf HK (1993) Ancient and new lime mortars – the correlation between their composition structure and properties. In: MJ THIEL ed, *Conservation of Stone and other Materials* London.pp 605-612. ISBN: 0-419-18410-4

Schueremans L, Cizer O, Janssens E, Serre G, Van Balen K (2011) Characterization of repair mortars for the assessment of their compatibility in restoration projects: Research and practice. *Constr Build Mater* 25:4338-4350. DOI: 10.1016/j.conbuildmat.2011.01.008

Sickels LB (1981) Organics vs, synthetics: their use as additives in mortars in Mortars cements and grouts used in the conservation of historic buildings. Symposium Rome 3–6 November 1981. Pp. 25–52. ICCROM Rome.

Sonninen E, Jungner H (2001) An improvement in preparation of mortar for Radiocarbon dating. *Radiocarbon* 43:271–273. DOI: 10.1017/S0033822200038108

Spensley E (2004) *Micromorphology of Construction and Culture at Trinidad de Nosotros, Peten, Guatemala*. M.A. Ph.D., Department of Archaeology, Boston University, Boston.

Stefanidou M (2010) Methods for porosity measurement in lime-based mortars. *Constr Build Mater* 24:2572–2578. DOI: 10.1016/j.conbuildmat.2010.05.019

1 Stella G, Fontana D, Gueli AM, Troja SO (2013) Historical mortars dating from OSL signals of fine grain
2 fraction enriched in quartz. *Geochronometria* 40:153–164. DOI: 10.2478/s13386-013-0107-8

3
4 Stella G, Almeida L, Basilio L, Pasquale S, Dinis J, Almeida M, Gueli AM (2018) Historical building dating:
5 a multidisciplinary study of the convento de São Francisco (Coimbra, Portugal). *Geochronometria*
6 45:119-129. DOI: 10.1515/geochr-2015-0089

7
8
9
10 Štukovnik P, Marinšek M, Bokan-Bosiljkov V (2016) Long term influence of ACR on lime-based mortars.
11 Properties. *Proceedings of the 4th Historic Mortars Conference HMC2016*. Santorini. Greece. pp. 300-
12 306. ISBN:9609992234

13
14
15 Švarcová S, Hradil D, Hradilová J, Čermáková Z (2021) Pigments – Copper-based greens and blues.
16 *Archaeol Anthropol Sci* (this Topical Collection)

17
18
19 Thomson ML, Lindqvist J-E, Elsen J, Groot CJWP (2004) Porosity of Mortars. In: "Characterization of Old
20 Mortars with Respect to Repair- Final Report of RILEM TC 167-COM. pp.76-106. DOI:
21 10.1617/2912143675.006

22
23
24
25 Toffolo MB, Ricci G, Caneve L, Kaplan-Ashiri I (2019) Luminescence reveals variations in local structural
26 order of calcium carbonate polymorphs formed by different mechanisms. *Scient Rep* 9:16170. DOI:
27 10.1038/s41598-019-52587-7

28
29
30
31 Toffolo MB, Ricci G, Chapoulie R, Caneve L, Kaplan-Ashiri I (2020) Cathodoluminescence and laser-
32 induced fluorescence of calcium carbonate: a review of screening methods for radiocarbon dating of
33 ancient lime mortars. *Radiocarbon* 62:545–564. DOI: 10.1017/RDC.2020.21

34
35
36
37 Tunçoku SS, Caner-Saltık EN (2006) Opal-A rich additives used in ancient lime mortars. *Cem Concr Res*
38 36:1886-1893. DOI: 10.1016/j.cemconres.2006.06.012

39
40
41 Urbanová P, Hourcade D, Ney C, Guibert P (2015) Sources of uncertainties in OSL dating of
42 archaeological mortars: the case study of the Roman amphitheatre Palais-Gallien in Bordeaux. *Radiat*
43 *Meas* 72:100–110. DOI: 10.1016/j.radmeas.2014.11.014

44
45
46
47 Urbanová P, Guibert P (2017) A methodological study on single grain OSL dating of mortars:
48 comparison of five reference archaeological sites. *Geochronometria* 44:77–97. DOI: 10.1515/geochr-
49 2015-0050

50
51
52
53 Urbanová P, Michel A, Bouvier A, Cantin N, Guibert P, Lanos P, Dufresne P, Garnier L (2018) Novel
54 interdisciplinary approach for building archaeology: integration of mortar luminescence dating into
55 archeological research an example of Saint Seurin basilica Bordeaux. *J Archaeol Sci R* 20:307–323. DOI:
56 10.1016/j.jasrep.2018.04.009.
57
58
59
60
61
62
63
64
65

1 Urbanová P, Boaretto E, Artioli G (2020) The state-of-the-art of dating techniques applied to ancient
2 mortars and binders: a review. Radiocarbon 62:503–525. DOI: 10.1017/RDC.2020.43

3
4 Válek J, Hughes JJ, Groot CJWP (2012) A State-of-the-Art Summary, In: Historic mortars:
5 characterisation, assessment and repair, Válek J, Hughes JJ, Groot CJWP, Edts., RILEM Bookseries,
6 volume 7: 1-12. DOI: 10.1007/978-94-007-4635-0

7
8
9
10 Valek J, Hughes J J, Groot Caspar JWP (Eds.) (2012) Historic Mortars Characterisation. Assessment and
11 Repair RILEM Bookseries. ISBN 978-94-007-4635-0

12
13
14 Van Strydonck M, Dupas M (1991) The classification and dating of lime mortars by chemical analysis
15 and Radiocarbon dating: a review. In: Waldren WH, Ensenyat JA, Kennard RC, editors, Second Deya
16 International Conference of Prehistory, Volume II, BAR International Series 574: 5–43. DOI:
17 10.1017/S0033822200041898

18
19
20
21 Van Strydonck M, Dupas M, Dauchot-Dehon M, Pachiaudi CJ, Marechal (1986) The influence of
22 contaminating carbonate and the variations of $\delta^{13}\text{C}$ in mortar dating. Radiocarbon 28:702–710. DOI:
23 10.1017/S003382220000792X

24
25
26
27 Varas MJ, Álvarez de Buergo M, Fort R (2005) Natural cement as precursor of Portland cement:
28 methodology for its identification. Cem Concr Res 35: 2055-2065. DOI:
29 10.1016/j.cemconres.2004.10.045

30
31
32
33 Varas MJ, de Buergo MA, Fort R (2007) The origin and development of natural cements: The Spanish
34 experience. Constr Build Mater 21:436-445. DOI: 10.1016/j.conbuildmat.2005.07.011

35
36
37
38 Varas-Muriel MJ (2012) Técnicas de caracterización petrológicas (II): microscopía óptica de
39 fluorescencia (MOF) y microscopía electrónica de barrido (MEB). En: La conservación de los
40 geomateriales utilizados en el patrimonio. Ed. Programa Geomateriales. Comunidad de Madrid,
41 España. 31-36. ISBN: 978-8461576609

42
43
44
45 Veiga R (2017) Air lime mortars: what else do we need to know to apply them in conservation and
46 rehabilitation interventions? A review. Constr Build Mater 157:132–140. DOI:
47 10.1016/j.conbuildmat.2017.09.080

48
49
50
51 Velosa AL, Veiga R, Coroado J, Ferreira VM, Rocha F (2010) Characterization of Ancient Pozzolan
52 Mortars from Roman Times to the 19th Century: Compatibility Issues of New Mortars with Substrates
53 and Ancient Mortars. In: DAN, M. B., PŘIKRYL, R. & TÖRÖK, Á. (eds.) Materials, Technologies and
54 Practice in Historic Heritage Structures. Dordrecht: Springer Netherlands., Chapter 13, pp. 235-257.
55
56
57
58 DOI: 10.1007/978-90-481-2684-2_13

1 Vitti P (2021) Mortars and masonry - Structural lime and gypsum mortars in Antiquity and Middle Ages.
2 Archaeol Anthropol Sci (this Topical Collection)

3
4 Ventolà L, Vendrell M, Giraldez P, Merino L (2011) Traditional organic additives improve lime mortars:
5 new old materials for restoration and building natural stone fabrics. Constr Build Mater 25:3313-3318.
6 DOI: 10.1016/j.conbuildmat.2011.03.020.
7

8
9 Walkden GM, Berry JR (1982). Natural calcite in cathodoluminescence - crystal-growth during
10 diagenesis. Nature 308:525-527. DOI: 10.1038/308525a0
11

12
13 Wallace W (1865) On ancient mortars. Journal of the Franklin Institute 79:409-411.
14

15
16 Wilhelm K, Viles H, Burke Ó (2016) Low impact surface hardness testing (Equotip) on porous surfaces—
17 advances in methodology with implications for rock weathering and stone deterioration research.
18 Earth Surf Proc Land 41:1027-1038. DOI: 10.1002/esp.3882
19

20
21 Yang FW, Zhang BJ, Pan CC, Zeng YY (2009) Traditional mortar represented by sticky rice lime
22 mortar—One of the great inventions in ancient China. Sci China Ser E-Tech Sci, Jun. 2009, vol. 52, no.
23 6, 1641-1647, doi: 10.1007/s11431-008-0317-0
24

25
26 Zacharias N, Mauz B, Michael CT (2002) Luminescence quartz dating of lime mortars, A first research
27 approach. Radiat Prot Dosim 101:379–382. DOI: 10.1093/oxfordjournals.rpd.a006006
28

29
30 Zhang K, Rampazzi L, Riccardi MP, Sansonetti A, Grimoldi A (2018) Mortar mixes with oxblood:
31 historical background, model sample recipes and properties. Adv. Geosci., 45, 19–24, 2018
32 <https://doi.org/10.5194/adgeo-45-19-2018>
33
34
35
36
37
38
39
40
41
42
43
44
45
46
47
48
49
50
51
52
53
54
55
56
57
58
59
60
61
62
63
64
65